its replication and transcription.[26,27] The N, P, and L proteins are assembled into the ribonucleoprotein, which is the viral replication unit. Therefore, we reasoned that combining a safe targeted therapy mechanism that destroys the host antiviral genetic program and enhances viral genome replication in cancer cells would generate a novel and innovative cancer gene therapy.

In this study, we generated a newly engineered MV, MV-NPL, which is based on the Edm tag strain but is armed with the *N*, *P*, and *L* genes of the wild-type strain. We demonstrated that MV-NPL has enhanced oncolytic activity against human renal cell carcinoma (RCC) cell lines *in vitro* and *in vivo* compared to MV-Edm tag and MV-P. We found that MV-NPL had faster replication and transcription than MV-Edm tag and MV-P in RCC cell lines *in vitro* and RCC cell line xenografts *in vivo*. In addition, MV-NPL efficiently proliferated and killed RCC cell line even in the presence of IFN-α. Furthermore, this oncolytic activity was specific as MV-NPL caused minimal cytopathic effects in normal human cell line.

RESULTS

CD46 is overexpressed in human RCC cell lines

CD46 expression in the human RCC cell lines A-498 and OS-RC-2, primary human RCC cells of T5, normal human skin fibroblast cell line BJ-1 was analyzed by flow cytometry. CD46 was expressed on the surface of most human RCC cell lines and primary human RCC cells: 93.8% in A-498, 93.7% in OS-RC-2, and 92–95% in primary human RCC cells (n = 3). However, only 8.7% in BJ-1 demonstrated positive expression of CD46 (**Figure 1**). These results demonstrated that human RCC cell lines and primary RCC cells expressed higher levels of CD46 than normal cells.

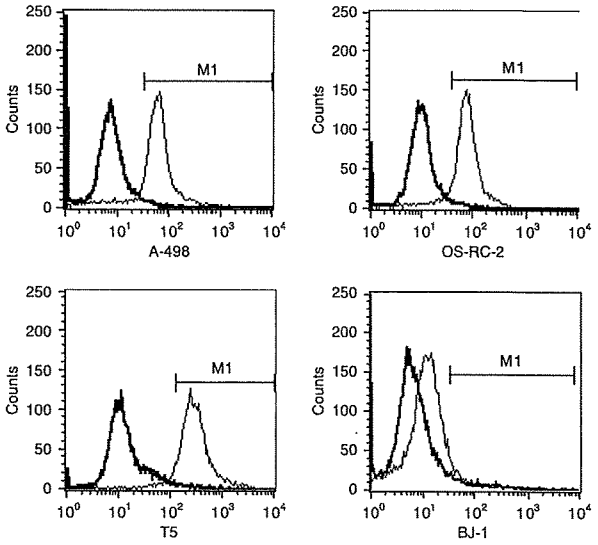

Figure 1 CD46 receptor expression on the human renal cell carcinoma (RCC) cell lines A-498 and OS-RC-2, primary human RCC cells of T5, and normal human cell line BJ-1. CD46 receptor was highly expressed on the human RCC cell lines A-498 and OS-RC-2 as well as primary human RCC cells of T5, but was minimally expressed on the normal human cell line BJ-1. The analysis was performed by flow cytometry. CD46 expression in isotype control is 1%. The thick histograms show the measured fluorescence of cells incubated with an isotype control (detailed) and the thin histograms represent cells labeled with an anti-CD46 fluorescein isothiocyanate antibody.

MV-NPL induces stronger CPEs than MV-P and MV-Etag in human RCC cell lines and primary human RCC cells

Schematic representation of the genome of MV-Etag (a V-defective vaccine-lineage strain) strain, engineered MV-Etag strain that expresses the wild-type *P* gene (MV-P) and the engineered MV-Etag strain that expresses the wild-type *N*, *P*, and *L* genes (MV-NPL) is shown in **Figure 2a**. They were rescued and efficiently propagated in Vero cells and used for the following experiments. We studied the CPEs associated with each MV in the human RCC cell lines A-498 and OS-RC-2, primary RCC cells (n = 3), the normal human skin fibroblast cell line BJ-1. Cells were infected with the various viruses at multiplicities of infection (MOIs) of 1 and 0.1 for 120 hours and the stained with crystal violet. Compared to MV-P and MV-Etag, MV-NPL demonstrated more dramatic CPEs in an MOI-dependent manner (n = 3; **Figure 2b**). The CPEs appeared at 72 hours postinfection with each MV at an MOI of 0.1 in both A-498 and OS-RC-2 cells and primary RCC cells (data not shown). However, normal human cell line BJ-1 showed minimal CPEs after each MV infection (**Figure 2b**). We further determined the cell viability after infection with the various viruses using the Cell-Titer 96 Aqueous Non-Radioactive Cell Proliferation Assay. Analyses were performed every 24 hour for 120 hours. Compared with MV-P and MV-Etag, MV-NPL demonstrated a greater reduction of proliferation in A-498, OS-RC-2, and primary RCC cells from 72 or 96 hours to 120 hours at an MOI of 0.1 (n = 3; **Figure 2c**).

MV-NPL induces faster cell lysis in A-498 cells than MV-P and MV-Etag

A-498 cells were plated in 6-well plates at a density of 2×10^5 cells/well. The cells were infected with various viruses at an MOI of 0.1 and the supernatants and cells were collected from 12 to 120 hours. The intracellular viruses were released by two cycles of freezing/thawing. The viral titers were determined as the TCID50 (50% tissue culture infective dose) in Vero cells in a 96-well plate. The intracellular MV-NPL viral titer of A-498 cells peaked at 60 hours postinfection (**Figure 3a**). Compared with MV-NPL, intracellular MV-P virus demonstrated slower replication and the viral titer peaked at 84 hours (**Figure 3a**). In the culture supernatant, the MV-NPL viral titer peaked at 72 hours (**Figure 3b**). Similar to the intracellular viral titer, the extracellular MV-P titer peaked with delayed kinetics at 84–96 hours compared to MV-NPL. We also found that after the intracellular viral titer peaked, the viral titer in the culture supernatant peaked in A-498 cells infected with MV-NPL. Real-time RT-PCR analyses revealed a time-dependent increase in measles viral mRNA in A-498 cells, and compared with other viruses, cells infected with MV-NPL demonstrated higher viral mRNA levels (**Figure 3c**).

MVs induced human IFN-α production from human normal skin fibroblast cells of BJ-1, and human RCC cells of A-498 and OS-RC-2. MV-NPL more effectively evaded to the antiviral defense of IFN-α in Vero cells than MV-P and MV-Etag.

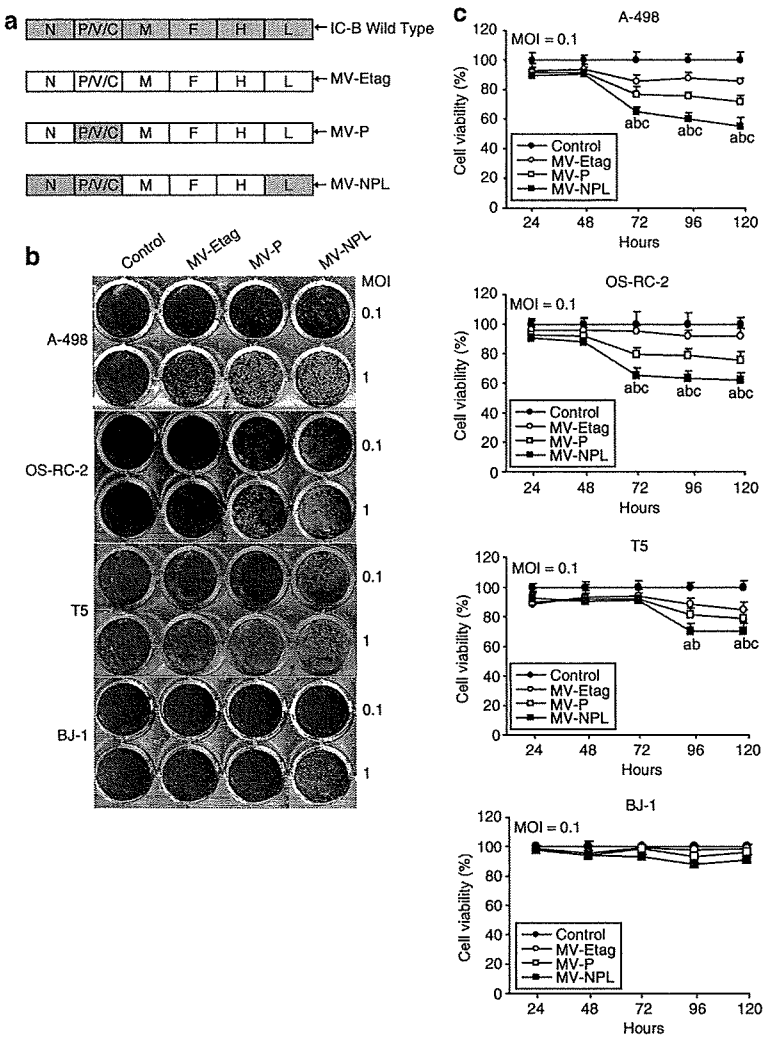

Figure 2 Induction of cytopathic effects (CPEs) and cell death in human renal cell carcinoma (RCC) cell lines A-498, OS-RC-2, primary RCC cells T5, and normal human cell line BJ-1 by MV-Etag, MV-P, and MV-NPL. (**a**) At 120 hours after infection with each MV at multiplicities of infection (MOIs) of 1 and 0.1, the cells were stained with crystal violet. (**b**) Cells were infected with each MV at an MOI of 0.1 and cell viability was analyzed using the MTT assay. Each value is normalized to the control (untreated cells), which was set at 100%, and represents the mean ± SD (**a**, $P < 0.01$, MV-NPL versus control group; **b**, $P < 0.01$, MV-NPL versus MV-Etag group; **c**, $P < 0.01$, MV-NPL versus MV-P group).

The IFN family, particularly type I IFN (IFN-α/β), induces a powerful innate antiviral response. IFN-α production induced by human normal and tumor cells after infection by MVs was quantified using IFN-specific enzyme-linked immunosorbent assay (ELISA) kits (**Figure 4a**). We examined the sensitivity of the MV viruses to human IFN-α. Vero cells were infected with different MVs at an MOI of 0.001, and then treated with human IFN-α (1,000 IU/ml) 2 hours after infection. The viral titers were determined at 48 hours postinfection. Human IFN-α effectively inhibited MV-Etag proliferation (**Figure 4b**). To some extent, IFN-α also suppressed MV-P proliferation, whereas it had no apparent effect on MV-NPL proliferation (**Figure 4b**). To investigate whether IFN-α can prevent the CPEs of MV, OS-RC-2 cells were infected with each MV at an MOI of 0.1. Different concentrations of human IFN-α (250–2,000 IU/ml) were added to the infected cells and crystal violet staining was performed at 120 hours after infection. Compared to MV-P and MV-Etag, MV-NPL more effectively induced CPE even in the presence of IFN-α. However, there were no obvious CPEs in BJ-1 cells (**Figure 4c**).

MV-NPL induces more apoptosis in human RCC cells than MV-P and MV-Etag

A-498 cells were infected with each MV at an MOI of 0.1, and apoptotic cells were analyzed by propidium iodide staining and subsequent flow cytometry. Upon infection with the MVs, the number of cells in sub-G1 increased in a time-dependent manner (**Figure 5a**). MV-NPL induced apoptosis in ~20 and 40% of cells at 48 and 72 hours at an MOI of 0.1, respectively (**Figure 5a**). However, at the same time points, MV-P and MV-Etag only induced apoptosis in ~10 and 15% of cells (**Figure 5a**). We further examined poly(ADP-ribose) polymerase expression and found that the 85-kd cleaved poly(ADP-ribose) polymerase fragment

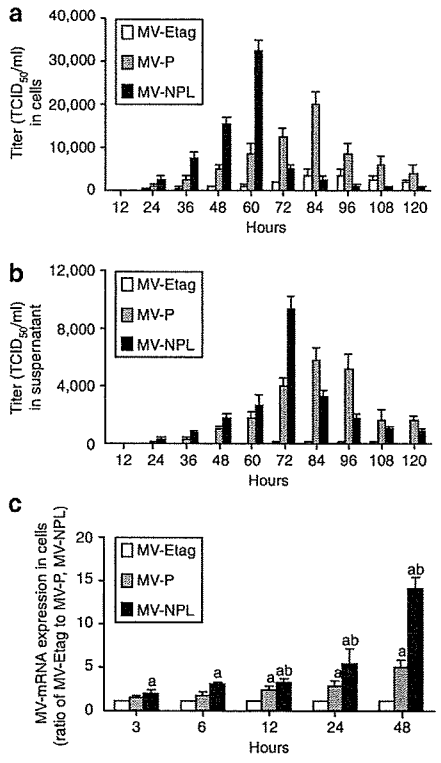

Figure 3 Production of MV-Etag, MV-P, or MV-NPL in the human renal cell carcinoma (RCC) cell line A-498. Cells were infected with each MV at an multiplicity of infection (MOI) of 0.1. (**a**) Cells and (**b**) supernatants were harvested at the indicated times. The viral titers were determined on Vero cells and expressed as $TCID_{50}$/ml. (**c**) Total RNA from A-498 cells was isolated at the indicated times. The viral mRNA levels were measured using real-time PCR. Each value is normalized to that in MV-Etag, which was set a ratio = 1, and represents the mean ± SD (**a**, $P < 0.05$, MV-NPL and MV-P versus MV-Etag; **b**, $P < 0.05$, MV-NPL versus MV-P). $TCID_{50}$, 50% tissue culture infective dose.

(85 kd) was more rapidly expressed in A-498 cells infected with MV-NPL than those infected with MV-P or MV-Etag (**Figure 5b**).

Intratumoral administration of MV-NPL induces regression of A-498 xenografts

Each MV was given intratumorally to nude mice bearing established (0.5–0.6 cm in diameter) subcutaneous human A-498 tumor xenografts. Intratumoral administration of MV-Etag or MV-P (10 doses of 1.0×10^5 $TCID_{50}$/dose) effectively suppressed the growth of A-498 xenografts. Compared with MV-Etag or MV-P, intratumoral injection of MV-NPL caused even more regression of the A-498 xenografts (**Figure 6a**). At 80 days after injection, the survival rate was significantly improved in the MV-NPL-injected group (55%), compared to the control group (0%), MV-Etag-injected group (0%), and MV-P-injected group (11%) (**Figure 6b**). A-498 xenografts infected with MV-NPL had the highest mRNA expression of the *M* gene of MV, indicating that MV-NPL was more effectively replicated in the xenografts than MV-P at 19 days after the injection when the former significantly suppressed the tumor growth than the latter ($P < 0.05$) (**Figure 6c**).

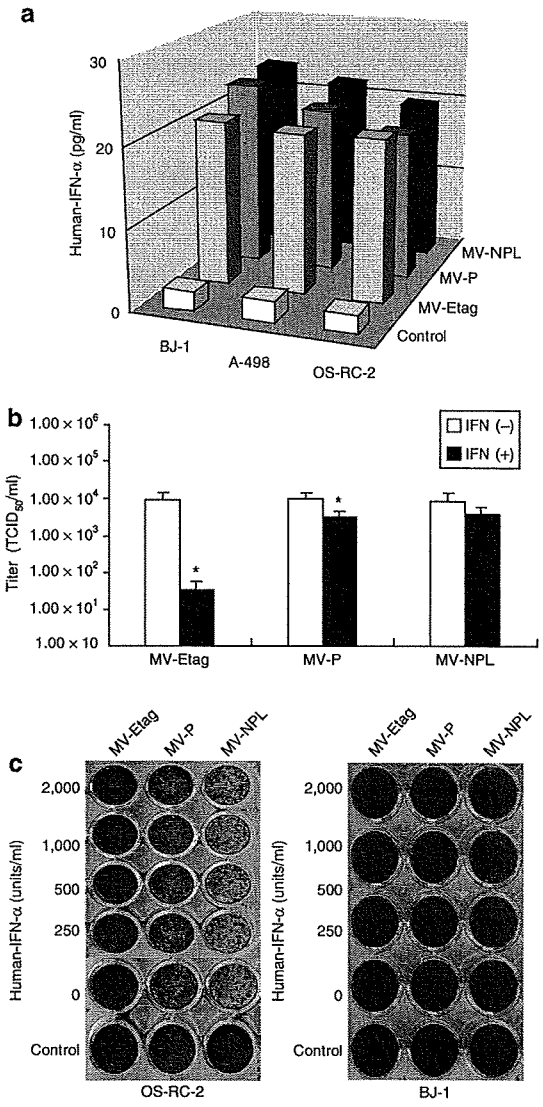

Figure 4 Different sensitivities of MV-Etag, MV-P, and MV-NPL to human INF-α. (**a**) BJ-1, A-498 and OS-CR-2 cells were infected with MV-Etag, MV-P, or MV-NPL at an multiplicity of infection (MOI) of 0.1. After 48-hour infection, the production of IFN-α was determined using human IFN-α enzyme-linked immunosorbent assay kit. (**b**) Vero cells were infected with each MV at an MOI of 0.001 and cultured in the presence or absence of 1,000 IU/ml recombinant IFN-α. Viral titers at 48 hours were determined by titrating the TCID50 on Vero cells, $*P < 0.05$ versus IFN(+). (**c**) OS-RC-2 cells and BJ-1 cells in 24-well plates were infected with each MV at an MOI of 0.1. Two hours after infection, human IFN-α was added to the cells at the indicated concentrations. At 120 hours after infection, the cells were stained with crystal violet. IFN, interferon; $TCID_{50}$, 50% tissue culture infective dose.

DISCUSSION

Oncovirotherapy using replication-competent viruses for cancer treatment has recently attracted considerable attention. Engineering replication-competent viruses for cancer therapy is a novel and promising strategy. Live-attenuated MV has a potent and tumor-specific oncolytic activity against a variety of human tumors.[9,13,28,29] In clinical trials, the MV vaccine strain has been shown to mediate regression of T-cell lymphomas when administered intratumorally.[11]

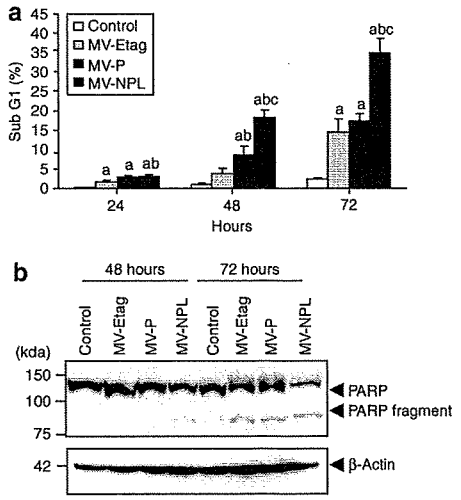

Figure 5 Apoptosis induced by MV-Etag, MV-P or MV-NPL in the human renal cell carcinoma (RCC) cell line A-498. Cells were infected with each MV at an multiplicity of infection (MOI) of 0.1. (**a**) Adherent and detached cells were harvested at 24, 48, and 72 hours postinfection. The percentage of sub-G1 cells was measured by fluorescence-activated cell sorting (**a**, $P < 0.05$, MV-NPL, MV-P and MV-Etag versus control; **b**, $P < 0.05$, MV-NPL and MV-P versus MV-Etag; **c**, $P < 0.05$, MV-NPL versus MV-P). (**b**) Whole-cell lysates of A-498 cells that were infected with each MV were subjected to western blot analysis using anti-PARP and β-actin antibodies. PARP, poly(ADP-ribose) polymerase.

However, there is no report on the oncolytic effects of measles virus on human RCCs. In this study, we report for the first time that measles virus has potent antitumor activity against human RCC cells *in vitro* and in *vivo*.

Numerous factors in the tumor microenvironment, such as the stromal architecture and surrounding innate immune system, could potentially restrict viral replication and spread *in vivo*.[30] Human type I IFNs such as IFN-α/β have been shown to inhibit gene expression and the production of progeny virions of the measles virus vaccine strain, including Edmonston tag strain.[31–33] In order to more effectively control tumor growth and eventually eradicate tumors by direct viral spread and oncolysis, an attenuated replication-competent virus must be able to evade the host innate immune response.[13,34] The P/V/C protein of the MV wild-type strain encoded by the *P* gene was shown to block IFN-α induced-signaling, allowing the virus to evade the innate immune response.[13,18,31,35,36] The N, P and L proteins assemble into the ribonucleoprotein, which serves as the MV replication unit. In our study, we found that wild-type N protein provided virus with resistance to IFN similar to P (data no shown). Moreover, the L protein gene of wild type can more effectively induce viral RNA and protein synthesis than vaccine strain.[37] In this study, we engineered a novel MV-Edm by replacing the *N*, *P*, and *L* genes with those of the wild-type MV strain to create a virus that rapidly replicates on human renal cancer cells. Compared to MV-P and MV-Etag, MV-NPL exhibited more efficient replication and a potent killing effect in human renal cancer cells *in vitro* and *in vivo*. In our study, we demonstrated that human IFN-α effectively inhibited the replication of MV-Etag and MV-P, but not MV-NPL, at an MOI of 0.001 in Vero cells *in vitro*. Furthermore, MV-NPL exhibited more efficient cytopathic effects than MV-Etag and MV-P in OS-RC-2 cells even in the presence of IFN-α.

Several mechanisms could account for the enhanced antitumoral effects of the engineered virus *in vitro*, such as faster replication kinetics, enhanced cell killing, or evasion of host antiviral mechanisms.[13,34] In this study, we demonstrated that MV-NPL replicated faster than MV-P and MV-Etag. In addition, RCCs infected with MV-NPL produced more viruses than those infected with MV-P or MV-Etag. Measles M mRNA was detected earlier in A-498 cells infected with MV-NPL than with MV-P or MV-Etag, which resulted in more substantial upregulation of viral protein production compared to the other viruses in a time-dependent manner (**Figure 3**). Therefore, we considered that the rapid oncolysis of cancer cells induced by MV-NPL is due to rapid viral mRNA transcription followed by abundant intracellular viral protein production and accelerated cancer cells lysis, causing the cells to necrose after viral infection. To determine the mechanism of MV-induced cell death, we used sub-G1 staining. Our results demonstrated that MV-NPL induced apoptosis in infected tumor cells faster than MV-Etag and MV-P. Therefore, we concluded that not only necrosis but also apoptosis was an important mode in MV-induced cell death.

MV has been shown to use two receptors, SLAM (CD150) and CD46, for entry into cells. SLAM (CD150) is a signaling lymphocyte activation molecule and its expression profile is confined to immune cells. CD46 is ubiquitously expressed in nucleated cells. The MV-Edm strain can infect cells via CD46, which is expressed more frequently in human cancer cells than normal cells. The most important issue to consider when developing an effective oncovirotherapy is that the oncolytic virus needs to selectively infect tumor cells but not normal cells. Our data demonstrated that CD46 was overexpressed in human RCC cell lines as well as cultured primary human RCC cells with 11-fold higher expression than in the normal human BJ-1 cell line. Compared to cancer cells, MV induces minimal CPEs in normal human cell line. These results suggested that cancer cells are suitable targets for MV infection.

Compared with oncolytic DNA viruses, RNA viruses do not require host nuclear transcription factors, and must rely on an alternative mechanism to preferentially replicate in tumor cells.[30] Furthermore, the MV genome is very stable, and the vaccine strains have never reverted to pathogenic forms. The Edmonston strain has been successfully used as a vaccine with an excellent safety profile. These data suggest that the MV vaccine strain has high tumor selectivity and safety, even though additional safety studies should be performed before starting clinical trials. In this study, we demonstrated that even low intratumoral doses of the engineered MV *in vivo* are sufficient to induce tumor regression.

We also demonstrated that MV-NPL efficiently induced tumor regression and showed the highest viral mRNA expression in the mouse model compared to MV-Etag and MV-P. The oncolysis of cancer cells has been clearly shown *in vitro*, so we suspected that the same mechanism occurs in our *in vivo* model. In current oncolytic virus research, intratumoral, intravenous, or intraperitoneal injections have been used to treat immune-deficient mice bearing human tumor xenografts. Among these treatments, intratumorally injected virus can efficiently escape circulating

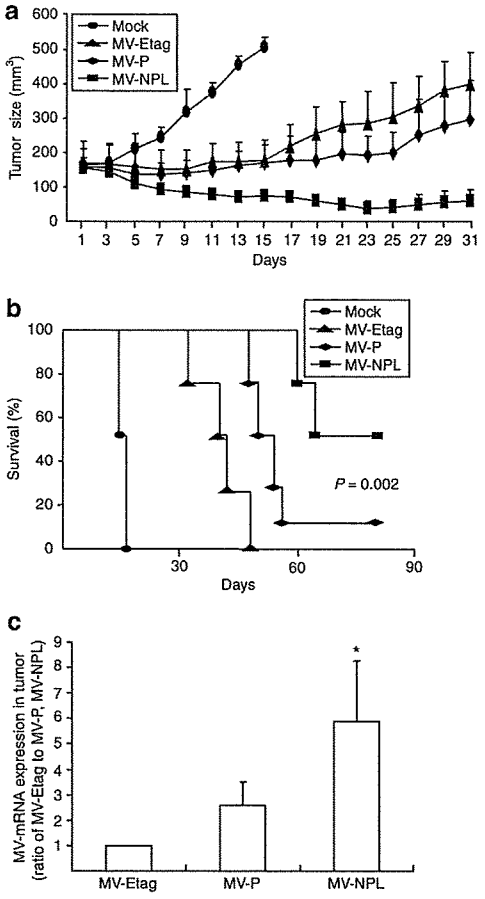

Figure 6 Therapeutic efficacy of MV-Etag, MV-P, or MV-NPL for renal cell carcinoma (RCC) xenografts *in vivo*. (**a**) A-498 cells (5×10^6 in 100 µl phosphate-buffered saline) were injected subcutaneously. When tumors reached a diameter of 0.5–0.6 cm, the virus was injected intratumorally every other day for a total of 10 doses (1.0×10^5 $TCID_{50}$/dose) over 19 days. The first day of injection represents day 1, and the tumor volumes were measured every other day ($n = 9$/group). (**b**) Kaplan–Meier survival analysis are shown for treated mice and mock-treated mice ($P = 0.002$, MV-NPL versus MV-P). (**c**) Intratumoral administration of each MV was initiated with a 1.0×10^5 $TCID_{50}$ injection. Nineteen days after injection, the tumors were harvested and the *M* gene viral mRNA levels were determined by real-time PCR, $^*P < 0.05$ versus MV-P. $TCID_{50}$, 50% tissue culture infective dose.

MV–neutralizing antibodies; therefore, this method is considered to be more desirable.

Currently, some additional immune mechanisms have been implicated in oncovirotherapy-mediated therapeutic effects. Several studies have shown that CD8 T cells are related to the efficiency of herpes simplex virus–induced,[38] vesicular stomatitis virus–induced,[39] and MV-induced[14,40] virotherapies. However, adult patients infected with measles virus have significantly higher levels of regulatory T cells, IFN-γ, and interleukin-10 (ref. 41). Furthermore, the phagocytosis of apoptotic MV-infected mesothelioma cells induced spontaneous DC maturation and activation and significant CD8 T-cell amplification. Collectively, oncovirotherapy may exhibit multiple clinical effects, including tumor lysis followed by the appearance and persistence of antitumor immunity.

In summary, our current results demonstrated that newly engineered MV-NPL has more effective oncolytic activity than the parental virus or MV-P as a systemic therapy for human RCC. The engineered virus caused CPEs in human RCCs, but had no toxic effects on normal human cells. Furthermore, MV-NPL replicated faster and more effectively resisted IFN-α than MV-Etag and MV-P, allowing the virus to escape the innate immune response. Although additional safety issues should be investigated, these properties of MV-NPL may help establish an innovative cancer therapy in the future.

MATERIALS AND METHODS

Construction of engineered viruses. The plasmids p(+)MV323 (ref. 42) and p(+)MV2A (ref. 43), which encode the full-length antigenomic complementary DNA of the IC-B wild-type strain and the Edmonston tag strain, respectively, were used in this study. We inserted restriction enzyme sites (*Sna*BI-N-*Spl*I-P-*Eco*47III-M-*Nru*I-F-*Pac*I-H-*Spe*I-L-*Pme*I) into the noncoding region of the p(+)MV323 genome using PCR with specific primers. Using the appropriate restriction enzymes, a series of genomic regions of p(+)MV2A were replaced with identical regions in p(+)MV323, which generated plasmids carrying the full-length genomes of recombinant engineered viruses (**Figure 3a**). Engineered MVs were rescued from cloned viral genome complementary DNA with a highly efficiently reverse genetics system as described previously.[44] The engineered MVs were propagated in Vero cells, an African green monkey kidney epithelial cell line, and passage three viral stocks were used in this study.

Cell line culture. The human RCC cell lines A-498 and OS-RC-2, the normal human skin fibroblast cell line BJ-1 were maintained in Dulbecco's modified Eagle's medium supplemented with 10% heat-inactivated fetal bovine serum (Japan Bioserum; Sigma, Steinheim, Germany). Vero cells were used to produce measles virus and maintained in Dulbecco's modified Eagle's medium supplemented with 5% heat-inactivated fetal bovine serum (Japan Bioserum). All media used in this study contained 100 U/ml of penicillin–streptomycin. All cell lines used in this study were cultured in a humidified atmosphere with 5% CO_2 at 37 °C.

Primary cell culture. Primary human RCC tissues were established using surgical specimens immediately after resection from Kyushu University Hospital after institutional review board approval and informed patient consent. Tissues were sliced, minced, treated with collagenase (GIBCO, Invitrogen, Carlsbad, CA) at 37 °C for 2 hours on a shaker, and then filtered through a nylon mesh (100-µm diameter) to obtain single cell suspensions. Harvested cells were cultured in Minimum Essential Medium α medium (GIBCO, Invitrogen) supplemented with 10% heat-inactivated fetal bovine serum (Hyclone, Logan, UT) and 4 µg/ml of Gentamicin Reagent Solution (GIBCO, Invitrogen). All cells used in this study were cultured in a humidified atmosphere with 5% CO_2 at 37 °C.

Flow cytometry. CD46 expression and the subdiploid status of cells (sub-G1) were determined by flow cytometry. To measure CD46 expression, the cells were harvested with Cell Dissociation Buffer (GIBCO, Invitrogen), washed twice with phosphate-buffered saline (PBS), and incubated with a fluorescein isothiocyanate–labeled monoclonal mouse anti-human CD46 or control antibodies (BD Biosciences, Pharmingen) for 1 hour on ice. The cells were washed twice with PBS and then 10,000 cells per sample were analyzed using a FACScan (BD Biosciences, San Jose, CA). For sub-G1, A-498 cells were plated in 6-well plates, and then treated with each MV at an MOI of 0.1. Adherent and detached cells were harvested at 24, 48, and 72 hours after infection and fixed in ice-cold 70% ethanol for at least 1 hour. Cell pellets were washed twice with PBS and then incubated for 30 minutes at room temperature in 1 ml PBS containing 50 µg propidium iodide (Sigma-Aldrich, St Louis, MO), 0.1% Triton X-100, 1 mmol/l

EDTA, and 0.5 mg RNaseA. After staining, 10,000 events per sample were analyzed using a FACScan (BD Biosciences). Fragmented apoptotic nuclei were recognized by their sub-G1 DNA content. The percentage of sub-G1 cells was recorded for each sample. All flow cytometry data were analyzed using the Mod Fit LT software (Verity Software House, Topsham, MN).

***Evaluation of CPEs* in vitro.** A-498, OS-RC-2, T5 (cultured primary human RCC cells), and BJ-1 cells were cultured in 24-well plates at a density of 2×10^4 cells/well. The cells were infected with each MV at an MOI of 1 or 0.1 in 0.2 ml of Opti-MEM I (GIBCO, Invitrogen) for 2 hours. The virus suspension was removed, and 1 ml of fresh medium was added to each well with or without the noted concentrations of human IFN-α. At 120 hours after infection, the cells were gently washed twice with PBS, and the remaining cells were fixed with 0.5% glutaraldehyde in PBS for 15 minutes. Then, cells were washed with PBS and stained with 0.1% crystal violet solubilized in 2% ethanol–distilled water. The stained product was subsequently washed twice with distilled water, air-dried, and then photographed.

Western blot analysis and ELISA. Infected cells were harvested and solubilized in a Nonidet P-40-based lysis buffer [20 mmol/l Tris (pH 7.4), 250 mmol/l NaCl, 1% Nonidet P-40, 1 mmol/l EDTA, 50 mg/ml leupeptin, and 1 mmol/l phenylmethylsulfonyl fluoride). After incubating on ice for 5 minutes, the cell lysates were clarified by centrifugation at 13,000 *g* for 30 minutes at 4 °C. The protein concentrations in the lysates were quantified using Multiskan spectrum. The samples were separated on precast 4–12% gradient MOPS polyacrylamide gels (NOVEX, San Diego, CA), and then transferred to nitrocellulose membranes (BIO-RAD, Hercules, CA). The membranes were pretreated with Tris-buffered saline containing 5% dry milk and 0.05% Triton X-100 (TBST) for 1 hour at room temperature and then incubated with monoclonal antiproteolytic cleavage of poly(ADP-ribose) polymerase (Biovision, Mountain View, CA) and a rabbit anti-β-actin (CHEMICON International, Temecula, CA) antibodies for 1 hour at room temperature. After several washes in TBST, the membranes were probed with rabbit or mouse peroxidase-conjugated secondary antibodies (Santa Cruz Biotechnology, Santa Cruz, CA) at room temperature for 1 hour. After a final wash with TBST, the immune-reactivity of the blots was detected using an enhanced chemiluminescence detection system (Amersham, Piscataway, NJ). ELISA specific for IFN-α was performed using a human IFN-α ELISA kit (PBL Biomedical Laboratories) as per manufacturer's instructions.

Cell proliferation assay. The Cell-Titer 96 Aqueous Non-Radioactive Cell Proliferation Assay (Promega, Madison, WI) was used in this study. A-498, OS-RC-2, T5, and BJ-1 cells were plated in 96-well plates at a density of 1×10^4 cells/well. Twelve hours after seeding, the cells were infected with each MV at an MOI of 0.1 for different time intervals and then incubated with 20 μl of MTS reagent for 2 hours at 37 °C. The absorbance at 490 nm was recorded using an ELISA plate reader.

Assessment of MV replication in a human RCC cell line. The human RCC cell line A-498 was seeded in 6-well plates at a density of 2.0×10^4 cells/well. Twelve hours after plating, the cells were infected with each MV at an MOI of 0.1 in Opti-MEM I. The cells and supernatants were collected at different time intervals. The viruses were released by two cycles of freezing and thawing. The viral titers in the cells and supernatants were determined by titrating the TCID50 on Vero cells.

Human IFN-α sensitivity of MVs. Vero cells were infected with each MV at an MOI of 0.001. Two hours after infection, human IFN-α A/D (Sigma, St Louis, MO) was added to the cells at a concentration of 1,000 IU/ml. At 48 hours postinfection, the cells were harvested together with the culture media. The viral titers in both the intracellular samples and the culture supernatants were determined by titrating the TCID50 on Vero cells.

In vivo *xenograft experiments.* A-498 cells (5×10^6 in 100 μl PBS) were injected subcutaneously into the right flanks of 4-week-old female BALB/c nude mice using a 27-gauge needle. The length and width of the tumors in each mouse were measured daily with calipers. Mice were randomly divided into four groups: MV-Etag, MV-P, MV-NPL, or control (n = 9/group). Intratumoral administration of each MV was initiated when the tumors reached a diameter of 0.5–0.6 cm. The mice were injected with each MV (1×10^5 TCID50 in 50 μl Opti-MEM I), and each mouse received 10 MV doses on days 1, 3, 5, 7, 9, 11, 13, 15, 17, and 19. Control mice (mock therapy group) were injected with equal volumes of Opti-MEM I containing no virus. The tumor volume was calculated as length × width × width/2. Mice were killed if they lost >20% of their body weight or the tumor diameter exceeded 1.0 cm. All mouse experiments were approved by the Committee of the Ethics on Animal Experiments in the Faculty of Medicine, Kyushu University and carried out following the Guidelines for Animal Experiments in the Faculty of Medicine, Kyushu University, Fukuoka, Japan and The Law and Notification of the Government.

Statistical analysis. Each experiment was repeated three different times, and data are presented as means ± SD. Where indicated, the data were analyzed by a one-way analysis of variance with Bonferroni's *post hoc* test using SPSS 15.0 software (SPSS, Chicago, IL). P values <0.05 were considered statistically significant.

ACKNOWLEDGMENTS

This work was supported by a grant from the Ministry of Education, Culture, Sports, Science and Technology.

REFERENCES

1. Cattaneo, R, Miest, T, Shashkova, EV and Barry, MA (2008). Reprogrammed viruses as cancer therapeutics: targeted, armed and shielded. *Nat Rev Microbiol* **6**: 529–540.
2. Kirn, DH and Thorne, SH (2009). Targeted and armed oncolytic poxviruses: a novel multi-mechanistic therapeutic class for cancer. *Nat Rev Cancer* **9**: 64–71.
3. Liu, TC and Kirn, D (2008). Gene therapy progress and prospects cancer: oncolytic viruses. *Gene Ther* **15**: 877–884.
4. Aghi, M and Martuza, RL (2005). Oncolytic viral therapies—the clinical experience. *Oncogene* **24**: 7802–7816.
5. Kim, M, Chung, YH and Johnston, RN (2007). Reovirus and tumor oncolysis. *J Microbiol* **45**: 187–192.
6. Nettelbeck, DM, Rivera, AA, Balagué, C, Alemany, R and Curiel, DT (2002). Novel oncolytic adenoviruses targeted to melanoma: specific viral replication and cytolysis by expression of E1A mutants from the tyrosinase enhancer/promoter. *Cancer Res* **62**: 4663–4670.
7. Connor, JH, Naczki, C, Koumenis, C and Lyles, DS (2004). Replication and cytopathic effect of oncolytic vesicular stomatitis virus in hypoxic tumor cells *in vitro* and *in vivo*. *J Virol* **78**: 8960–8970.
8. Csatary, LK, Gosztonyi, G, Szeberenyi, J, Fabian, Z, Liszka, V, Bodey, B *et al.* (2004). MTH-68/H oncolytic viral treatment in human high-grade gliomas. *J Neurooncol* **67**: 83–93.
9. Peng, KW, TenEyck, CJ, Galanis, E, Kalli, KR, Hartmann, LC and Russell, SJ (2002). Intraperitoneal therapy of ovarian cancer using an engineered measles virus. *Cancer Res* **62**: 4656–4662.
10. Fu, X, Tao, L and Zhang, X (2007). An oncolytic virus derived from type 2 herpes simplex virus has potent therapeutic effect against metastatic ovarian cancer. *Cancer Gene Ther* **14**: 480–487.
11. Heinzerling, L, Künzi, V, Oberholzer, PA, Kündig, T, Naim, H and Dummer, R (2005). Oncolytic measles virus in cutaneous T-cell lymphomas mounts antitumor immune responses *in vivo* and targets interferon-resistant tumor cells. *Blood* **106**: 2287–2294.
12. Vidal, L, Pandha, HS, Yap, TA, White, CL, Twigger, K, Vile, RG *et al.* (2008). A phase I study of intravenous oncolytic reovirus type 3 Dearing in patients with advanced cancer. *Clin Cancer Res* **14**: 7127–7137.
13. Haralambieva, I, Iankov, I, Hasegawa, K, Harvey, M, Russell, SJ and Peng, KW (2007). Engineering oncolytic measles virus to circumvent the intracellular innate immune response. *Mol Ther* **15**: 588–597.
14. Gauvrit, A, Brandler, S, Sapede-Peroz, C, Boisgerault, N, Tangy, F and Gregoire, M (2008). Measles virus induces oncolysis of mesothelioma cells and allows dendritic cells to cross-prime tumor-specific CD8 response. *Cancer Res* **68**: 4882–4892.
15. McDonald, CJ, Erlichman, C, Ingle, JN, Rosales, GA, Allen, C, Greiner, SM *et al.* (2006). A measles virus vaccine strain derivative as a novel oncolytic agent against breast cancer. *Breast Cancer Res Treat* **99**: 177–184.
16. Blechacz, B, Splinter, PL, Greiner, S, Myers, R, Peng, KW, Federspiel, MJ *et al.* (2006). Engineered measles virus as a novel oncolytic viral therapy system for hepatocellular carcinoma. *Hepatology* **44**: 1465–1477.
17. Peng, KW, Ahmann, GJ, Pham, L, Greipp, PR, Cattaneo, R and Russell, SJ (2001). Systemic therapy of myeloma xenografts by an attenuated measles virus. *Blood* **98**: 2002–2007.

18. Takeuchi, K, Kadota, SI, Takeda, M, Miyajima, N and Nagata, K (2003). Measles virus V protein blocks interferon (IFN)-α/β but not IFN-γ signaling by inhibiting STAT1 and STAT2 phosphorylation. *FEBS Lett* **545**: 177–182.
19. Dörig, RE, Marcil, A, Chopra, A and Richardson, CD (1993). The human CD46 molecule is a receptor for measles virus (Edmonston strain). *Cell* **75**: 295–305.
20. Naniche, D, Varior-Krishnan, G, Cervoni, F, Wild, TF, Rossi, B, Rabourdin-Combe, C *et al.* (1993). Human membrane cofactor protein (CD46) acts as a cellular receptor for measles virus. *J Virol* **67**: 6025–6032.
21. Tatsuo, H, Ono, N, Tanaka, K and Yanagi, Y (2000). SLAM (CDw150) is a cellular receptor for measles virus. *Nature* **406**: 893–897.
22. Anderson, BD, Nakamura, T, Russell, SJ and Peng, KW (2004). High CD46 receptor density determines preferential killing of tumor cells by oncolytic measles virus. *Cancer Res* **64**: 4919–4926.
23. Ong, HT, Timm, MM, Greipp, PR, Witzig, TE, Dispenzieri, A, Russell, SJ *et al.* (2006). Oncolytic measles virus targets high CD46 expression on multiple myeloma cells. *Exp Hematol* **34**: 713–720.
24. Naniche, D, Yeh, A, Eto, D, Manchester, M, Friedman, RM and Oldstone, MB (2000). Evasion of host defenses by measles virus: wild-type measles virus infection interferes with induction of α/β interferon production. *J Virol* **74**: 7478–7484.
25. Grandvaux, N, tenOever, BR, Servant, MJ and Hiscott, J (2002). The interferon antiviral response: from viral invasion to evasion. *Curr Opin Infect Dis* **15**: 259–267.
26. Bourhis, JM, Canard, B and Longhi, S (2006). Structural disorder within the replicative complex of measles virus: functional implications. *Virology* **344**: 94–110.
27. Hagiwara, K, Sato, H, Inoue, Y, Watanabe, A, Yoneda, M, Ikeda, F *et al.* (2008). Phosphorylation of measles virus nucleoprotein upregulates the transcriptional activity of minigenomic RNA. *Proteomics* **8**: 1871–1879.
28. Dingli, D, Peng, KW, Harvey, ME, Greipp, PR, O'Connor, MK, Cattaneo, R *et al.* (2004). Image-guided radiovirotherapy for multiple myeloma using a recombinant measles virus expressing the thyroidal sodium iodide symporter. *Blood* **103**: 1641–1646.
29. Phuong, LK, Allen, C, Peng, KW, Giannini, C, Greiner, S, TenEyck, CJ *et al.* (2003). Use of a vaccine strain of measles virus genetically engineered to produce carcinoembryonic antigen as a novel therapeutic agent against glioblastoma multiforme. *Cancer Res* **63**: 2462–2469.
30. Russell, SJ (2002). RNA viruses as virotherapy agents. *Cancer Gene Ther* **9**: 961–966.
31. Ohno, S, Ono, N, Takeda, M, Takeuchi, K and Yanagi, Y (2004). Dissection of measles virus V protein in relation to its ability to block α/β interferon signal transduction. *J Gen Virol* **85**(Pt 10): 2991–2999.
32. Shingai, M, Ebihara, T, Begum, NA, Kato, A, Honma, T, Matsumoto, K *et al.* (2007). Differential type I IFN-inducing abilities of wild-type versus vaccine strains of measles virus. *J Immunol* **179**: 6123–6133.
33. Haller, O, Kochs, G and Weber, F (2006). The interferon response circuit: induction and suppression by pathogenic viruses. *Virology* **344**: 119–130.
34. He, LF, Gu, JF, Tang, WH, Fan, JK, Wei, N, Zou, WG *et al.* (2008). Significant antitumor activity of oncolytic adenovirus expressing human interferon-β for hepatocellular carcinoma. *J Gene Med* **10**: 983–992.
35. Ramachandran, A, Parisien, JP and Horvath, CM (2008). STAT2 is a primary target for measles virus V protein-mediated α/β interferon signaling inhibition. *J Virol* **82**: 8330–8338.
36. Yokota, S, Saito, H, Kubota, T, Yokosawa, N, Amano, K and Fujii, N (2003). Measles virus suppresses interferon-α signaling pathway: suppression of Jak1 phosphorylation and association of viral accessory proteins, C and V, with interferon-α receptor complex. *Virology* **306**: 135–146.
37. Takeda, M, Ohno, S, Tahara, M, Takeuchi, H, Shirogane, Y, Ohmura, H *et al.* (2008). Measles viruses possessing the polymerase protein genes of the Edmonston vaccine strain exhibit attenuated gene expression and growth in cultured cells and SLAM knock-in mice. *J Virol* **82**: 11979–11984.
38. Bolt, G, Berg, K and Blixenkrone-Møller, M (2002). Measles virus-induced modulation of host-cell gene expression. *J Gen Virol* **83**(Pt 5): 1157–1165.
39. Schneider-Schaulies, J, Dunster, LM, Schneider-Schaulies, S and ter Meulen, V (1995). Pathogenetic aspects of measles virus infections. *Vet Microbiol* **44**: 113–125.
40. Niewiesk, S, Götzelmann, M and ter Meulen, V (2000). Selective *in vivo* suppression of T lymphocyte responses in experimental measles virus infection. *Proc Natl Acad Sci USA* **97**: 4251–4255.
41. Yu, XL, Cheng, YM, Shi, BS, Qian, FX, Wang, FB, Liu, XN *et al.* (2008). Measles virus infection in adults induces production of IL-10 and is associated with increased CD4+ CD25+ regulatory T cells. *J Immunol* **181**: 7356–7366.
42. Takeda, M, Takeuchi, K, Miyajima, N, Kobune, F, Ami, Y, Nagata, N *et al.* (2000). Recovery of pathogenic measles virus from cloned cDNA. *J Virol* **74**: 6643–6647.
43. Tahara, M, Takeda, M and Yanagi, Y (2005). Contributions of matrix and large protein genes of the measles virus Edmonston strain to growth in cultured cells as revealed by recombinant viruses. *J Virol* **79**: 15218–15225.
44. Radecke, F, Spielhofer, P, Schneider, H, Kaelin, K, Huber, M, Dötsch, C *et al.* (1995). Rescue of measles viruses from cloned DNA. *EMBO J* **14**: 5773–5784.

Stem Cell Rev and Rep
DOI 10.1007/s12015-010-9140-7

APOA-1 is a Novel Marker of Erythroid Cell Maturation from Hematopoietic Stem Cells in Mice and Humans

Tomoko Inoue · Daisuke Sugiyama · Ryo Kurita · Tatsuo Oikawa · Kasem Kulkeaw · Hirotaka Kawano · Yoshie Miura · Michiyo Okada · Youko Suehiro · Atsushi Takahashi · Tomotoshi Marumoto · Hiroyuki Inoue · Norio Komatsu · Kenzaburo Tani

Abstract The mechanism that regulates the terminal maturation of hematopoietic stem cells into erythroid cells is poorly understood. Therefore, identifying genes and surface markers that are restricted to specific stages of erythroid maturation will further our understanding of erythropoiesis. To identify genes expressed at discrete stages of erythroid development, we screened for genes that contributed to the proliferation and maturation of erythropoietin (EPO)-dependent UT-7/EPO cells. After transducing erythroid cells with a human fetal liver (FL)-derived lentiviral cDNA library and culturing the cells in the absence of EPO, we identified 17 candidate genes that supported erythroid colony formation. In addition, the mouse homologues of these candidate genes were identified and their expression was examined in E12.5 erythroid populations by qRT-PCR. The expression of candidate erythroid marker was also assessed at the protein level by immunohistochemistry and ELISA. Our study demonstrated that expression of the *Apoa-1* gene, an apolipoprotein family member, significantly increased as hematopoietic

Electronic supplementary material The online version of this article (doi:10.1007/s12015-010-9140-7) contains supplementary material, which is available to authorized users.

T. Inoue · R. Kurita · T. Oikawa · H. Kawano · Y. Miura · M. Okada · Y. Suehiro · A. Takahashi · T. Marumoto · H. Inoue · K. Tani (✉)
Department of Molecular Genetics,
Medical Institute of Bioregulation, Kyushu University,
3-1-1, Maidashi, Higashi-ku,
Fukuoka 812-8582, Japan
e-mail: taniken@bioreg.kyushu-u.ac.jp

T. Inoue
e-mail: yokotomo@bioreg.kyushu-u.ac.jp

R. Kurita
e-mail: k-ryo@brc.riken.jp

T. Oikawa
e-mail: oitatsullo@yahoo.co.jp

H. Kawano
e-mail: kawano@bioreg.kyushu-u.ac.jp

Y. Miura
e-mail: ymiura@bioreg.kyushu-u.ac.jp

M. Okada
e-mail: okadatch@bioreg.kyushu-u.ac.jp

Y. Suehiro
e-mail: suehiro@sentan.med.kyushu-u.ac.jp

A. Takahashi
e-mail: atsushi@sentan.med.kyushu-u.ac.jp

T. Marumoto
e-mail: marumoto@sentan.med.kyushu-u.ac.jp

H. Inoue
e-mail: hinoue@bioreg.kyushu-u.ac.jp

D. Sugiyama
Faculty of Medical Sciences, Department of Hematopoietic Stem Cells, SSP Stem Cell Unit, Kyushu University,
3-1-1, Maidashi, Higashi-ku,
Fukuoka 812-8582, Japan
e-mail: sugiyama@hsc.med.kyushu-u.ac.jp

K. Kulkeaw
Faculty of Medical Sciences, Department of Hematopoietic Stem Cells, SSP Stem Cell Unit, Kyushu University,
3-1-1, Maidashi, Higashi-ku,
Fukuoka 812-8582, Japan
e-mail: kkulkeaw@yahoo.com

N. Komatsu
Department of Transfusion Medicine and Stem Cell Regulation,
Juntendo University School of Medicine,
2-1-1, Hongo, Bunkyo-ku,
Tokyo 113-8431, Japan
e-mail: komatsun@juntendo.ac.jp

Published online: 08 April 2010

stem cells differentiated into mature erythroid cells in the mouse FL. The Apoa-1 protein was more abundant in mature erythroid cells than hematopoietic stem and progenitor cells in the mouse FL by ELISA. Moreover, *APOA-1* gene expression was detected in mature erythroid cells from human peripheral blood. We conclude that APOA-1 is a novel marker of the terminal erythroid maturation of hematopoietic stem cells in both mice and humans.

Keywords APOA-1 · Erythroid cell maturation · Fetal liver erythropoiesis · Library screening · Lentiviral cDNA library

Introduction

Hematopoiesis is the process in which pluripotent hematopoietic stem cells (HSCs) are generated, differentiated into specific progenitors, and ultimately matured into a variety of blood cell types (erythrocytes, megakaryocytes, lymphocytes, neutrophils, and macrophages) [1]. During embryonic development, HSCs emerge in the aorta-gonad-mesonephros (AGM) region and expand first in the fetal liver (FL) and then in the bone marrow (BM) [2–5]. Among these hematopoietic organs, the FL is a site of both HSC expansion and active erythropoiesis [6]. Erythropoiesis is the process by which a vast number of enucleated red blood cells (RBCs) are produced from hematopoietic stem cells (HSC) [7]. However, the molecular mechanisms underlying erythropoiesis have not been fully elucidated, largely because there are only a few molecular markers of terminal erythroid maturation in both mice and humans. To address this issue, we focused on the events that regulate the terminal erythropoiesis of HSCs to mature erythroid cells in order to identify novel markers of mature erythrocytes.

A previous study established a mouse embryonic (ES) cell-derived erythroid progenitor (MEDEP) cell line [8]. Although erythroblasts expressing the erythroid maturation marker Ter119 [9] (a protein that molecularly resembles glycophorin) can be generated from ES/iPS-derived MEDEP cells, most of these cells remained nucleated, indicating that they have failed to complete terminal maturation. Ter119 antigen is currently the only erythroid-specific marker in mice. However, Ter119 is expressed at many maturation stages, from erythroblasts to mature, circulating erythrocytes. Therefore, additional markers for mature erythrocytes are needed. Numerous attempts at generating vast quantities of enucleated erythrocytes have failed to efficiently give rise to fully functional erythrocytes in vitro. This may in part be due to the gaps in our understanding of the mechanisms that regulate erythropoiesis.

The cytokine erythropoietin (EPO) plays important roles in erythropoiesis by regulating erythroid cell differentiation, maturation, proliferation, and survival. Erythroid cells are highly dependent on EPO during early differentiation and maturation but lose this dependency and express lower levels of the erythropoietin receptor (EPOR) as they mature [10]. We hypothesized that EPO-independent signaling plays an important role in the terminal stages of erythropoiesis.

We previously established a system in which specific lentiviral gene transduction induced hematopoiesis from embryonic stem cells of a nonhuman primate common marmoset in the absence of bone marrow stromal cells [11]. In addition, we constructed a high-performance human fetal liver (FL)-derived cDNA lentiviral library as a tool to facilitate the discovery of novel genes that are involved in the expansion of HSCs, erythropoiesis and/or liver development [12]. During embryogenesis, the FL is the major site of hematopoiesis, particularly erythropoiesis. Therefore, the FL-derived cDNA lentiviral library that we constructed contains many genes that are involved in the differentiation and maturation of these lineages. The goal of this study was to identify novel genes that are involved in or expressed during EPO-independent terminal erythroid maturation. We identified APOA-1 as a novel marker of the maturation of hematopoietic stem cells into mature erythroid cells.

Materials and Methods

Cells

UT-7/EPO cells [13] (kindly provided by Dr. Komatsu) are an EPO-dependent cell line that was established from the bone marrow of a patient with acute megakaryoblastic leukemia. This cell line was cultured in Iscove's modified Dulbecco's medium (IMDM) supplemented with 10% fetal bovine serum (FBS) and 1 U/mL human recombinant EPO (R&D Systems, Minneapolis, MN) at 37°C in 5% CO_2.

Lentivirus Production

The previously generated human fetal liver-derived Entry cDNA library [12] was used in this study. Briefly, 34 μg ($1–2\times10^5$ cDNA clones) of the library was mixed with 20 μg of pCAG-HIVg/p and 20 μg of pCMV-VSVG-RSV-Rev as the packaging plasmids in 3.5 ml of FBS-free DMEM, and then 370 μl of 1 mg/ml polyethylenimine (PEI) was added to the mixture. After a 30-min incubation, the DNA/PEI complexes were dropped onto semi-

confluent 293 T cells in a T175 flask containing Opti-MEM medium and then incubated for 3 h. Next, these cells were cultured in DMEM containing 10% FBS. Virus-containing supernatants were harvested 4 days post transduction and concentrated by centrifugation (9,000 rpm, 6–8 h, 4°C). The virus pellet was resuspended in 1 ml of IMDM and used for overnight transduction of UT-7/EPO cells.

Transduction of the Lentiviral Library into UT-7/EPO Cells

UT-7/EPO cells were transduced with the viral cDNA library and cultured in methylcellulose semi-solid medium containing IMDM, 10% FBS, and P/S without EPO for one month. After this period, several colonies were harvested, and genomic DNA was isolated from each colony using the QIAamp DNA Micro Kit (Qiagen, Valencia, CA).

Genomic PCR and Sequence Analysis

The integrated cDNAs were PCR amplified using a forward primer (5′-TTCAGGTGTCGTGAACACGCTACCG-3′) and reverse primer (5′-CCTCGATGTTAACTCTAGAG GATCC-3′). The Expand Long Template PCR System (Roche, Basel, Switzerland) was used following the manufacturer's protocol. cDNAs that were cloned into the CSII-CMV-RfA vector were sequenced with the forward (5′-CAAGCCTCAGACAGTGG-3′) and reverse (5′-AGCG TATCCACATAGCG-3′) primers using a Big-Dye Terminator v3.1 Cycle sequencing kit (Applied Biosystems, Foster City, CA) and an ABI PRISM 3100 Genetic Analyzer (Applied Biosystems). The sequences were compared with the DNA database from the DNA Data Bank of Japan using BLAST.

Cell Culture and Sorting

The EPO-dependent UT-7/EPO cell line was established and cultured as previously reported [13]. C57BL6J mice and ICR mice were purchased from Nihon SLC. Twelve o'clock noon was considered to be 0.5 day postcoitum (dpc) for plugged mice. Fetal liver (FL) cells from a 12.5 dpc embryo were filtered through a 40 μM nylon mesh and washed with PBS. The cells were stained with a FITC-conjugated anti-mouse CD71 Ab (BD Biosciences), PE-conjugated anti-mouse Sca-1 Ab (BD Biosciences), APC-conjugated anti-mouse c-Kit Ab (BD Biosciences), PE-Cy7-conjugated anti-mouse CD45 Ab (eBioscience) and APC-Cy7-conjugated anti-mouse Ter119 Ab (eBioscience). The cells were sorted using a FACS Aria cell sorter (BDIS), and the data files were analyzed using FlowJo software (Tree Star, Inc.).

Human peripheral blood (PB) was obtained from healthy volunteers. The PB was stained with a FITC-conjugated anti-human CD45 Ab (eBioscience), PE-conjugated anti-GPA antibody (eBioscience) and APC-conjugated anti-human CD41 antibody (BD Bioscience). The cells were sorted using a FACS Aria cell sorter (BDIS), and the data files were analyzed using FlowJo software (Tree Star, Inc.).

All animal studies were approved by the Committee on Ethics in Animal Experiments of Kyushu University, and the human studies were approved by the Committee on Ethics in Human clinical samples of Kyushu University. All of these studies were performed following the guidelines of Kyushu University.

RNA Extraction and Real-time RT-PCR

Total RNA was isolated from FL cells of ICR embryos at 12.5 dpc or whole embryos at 10.5 dpc using the RNAqueous-4PCR kit (Ambion). Total RNA from human peripheral blood was isolated with the RiboPure Kit (Ambion). A high-capacity cDNA Archive kit (Applied Biosystems) was used to synthesize cDNA from RNA. The mRNA levels of various genes were analyzed by qRT-PCR using SYBR Green and gene-specific primers with the StepOnePlus real-time PCR system (Applied Biosystems). The mRNA level of each target gene was normalized to β-actin as an internal control.

Immunohistochemistry

Ter119-positive cells from 12.5 dpc FL cells were isolated by flow cytometry as described above. Cells were cytospun onto glass slides and air-dried. The cells were fixed in 1% PFA at room temperature (RT) for 10 min. Nonspecific binding was blocked by incubating the cells at RT for 30 min in a blocking solution containing 1% BSA and 0.05% Triton X-100 in PBS. The following antibodies were diluted in the blocking solution: rabbit anti-Apoa-1 (1:50, Santa Cruz Biotechnologies, Inc.). A donkey anti-rabbit IgG (H+L)-Alexa555 (1:250, Invitrogen) was used as secondary antibody and TOTO-3 (1:1500, Invitrogen) was added as a nuclear stain. Coverslips were mounted with fluorescent mounting medium (Dako), and the slides were examined using a confocal microscope (Olympus).

ELISA

c-Kit-positive cells and Ter119-positive cells were isolated by flow cytometry as described above. Proteins were extracted from the sorted cells using the Qproteome Mammalian Protein Preparation kit (Qiagen). To detect the Apoa-1 protein, a goat anti-Apoa-1 (0.8 μg/ml,

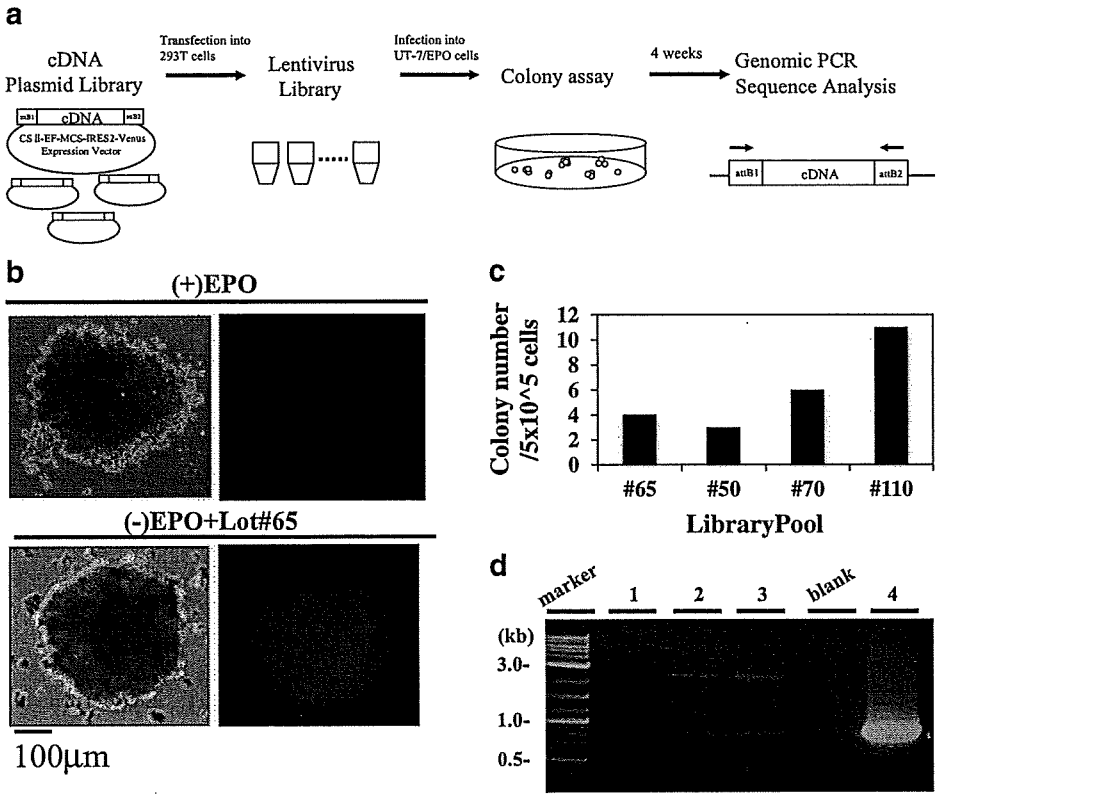

Fig. 1 Lentiviral human FL cDNA library screening in UT-7/EPO cells. **a** Strategy for identifying candidate EPO-independent regulators of erythropoiesis. Four pools (#65, #50, #70 and #110) of human FL-derived cDNA library were transfected into 293 T cells with helper plasmids to generate the lentiviral library. UT-7/EPO cells were transduced with these lentiviral library pools and then cultured in semisolid, EPO-deficient media for four weeks to positively select for clones that were able to form EPO-independent erythroid colonies. Finally, the cDNAs of the positive clones were sequenced to identify the transduced genes. **b** Erythroid colony assay. UT-7/EPO cells were transduced with the lentiviral pools (#65, #50, #70 and #110) and then transferred to semi-solid culture media. A representative colony derived from cells transduced with pool #65 is shown (Scale bar= 200 μm). A non-transduced colony was negative for Venus, while the lentiviral library-transduced colony was positive for Venus. **c** Colony number. A total of 22 colonies were obtained from UT-7/EPO cells that had been transduced with four lentiviral library pools and then analyzed by the colony formation assay. **d** Genomic PCR analysis. The inserted candidate genes were examined by genomic PCR using lentivirus insertion-specific primers. Lane 1: Untransduced UT-7/EPO cells (negative control), Lanes 2, 3: A colony derived from UT-7/EPO cells that had been transduced with lentiviral pool #65, Lane 4: GFP-transduced UT-7/EPO cells (positive control)

Rockland Immunochemicals) was used as a capture antibody, a rabbit anti-Apoa-1 (1:100, Santa Cruz Biotechnologies, Inc.,) was used as a detection antibody (primary antibody), and an anti-rabbit IgG-HRP (1:5000, Millipore) was used as the secondary antibody. Each antibody was captured onto 96-well immunoplates (Nunc) at 4°C for 16 h. Nonspecific binding was blocked by incubating the plate with 1% BSA/PBS for 2 h at RT. After the extracted proteins were added to the plate for 2 h at RT, the primary antibody was added for 1 h at RT, followed by the secondary antibody for 30 min at RT. The tetramethylbenzidine substrate was added to the wells for 30 min at RT, followed by a Stop Solution (R&D). The O.D. at 450 nm was measured using a Thermo Multiskan EX plate reader.

Results

Screening for Genes that Replace EPO/EPOR Signaling in UT-7/EPO Cells Using a Human FL Lentiviral Library

To identify novel genes that regulate erythroid cell maturation, we designed a strategy that monitored the ability of the EPO-dependent cell line, UT-7/EPO, to form erythropoietin (EPO)-independent colonies. Recently, we constructed a lentiviral human fetal liver (FL) cDNA library to search for novel genes that regulate hematopoiesis, including erythropoiesis [14]. Lentiviral cDNA library pools, which contained $1.32–1.98 \times 10^5$ cfu (colony forming units) per pool [14], were examined in this screen. We used the UT-7/EPO cell line, which is dependent upon EPO [13].

Table 1 Genes transduced in lentiviral-transduced erythroid colonies arising in the absence of Epo

Lentivirus pool #	Gene symbol	Discription
65	Angiotensinogen	AGT
	Estrogen receptor binding site associated antigen 9	EBAG9
50	B-cell CLL/lymphoma 2-like 1	BCL2-like 1
	Apolipoprotein A-1	APOA-1
70	ferritin heavy subunit	FHS
	3-phosphoinositide dependent protein kinase-1	PDPK1
	abl interactor 2	ABI-2
	Fibrinogen like 1	FGL1
	Apolipoprotein E	APOE
	Interferon induced transmembrane protein 2	1-8D
110	Asialoglycoprotein receptor 2	ASGR2
	Ferritin light chain	FLC
	Solute carrier family 27 (fatty acid transporter)	SLC27A2
	Ribosomal protein L10	RPL10
	Collagen type XVIII alpha 1	COL18A1
	Apolipoprotein J	APOJ
	Group-specific component	GC

When UT-7/EPO cells are transduced with genes in this lentiviral library that can functionally replace EPO/EPOR signaling, expression of these genes will result in colony formation in the absence of EPO (Fig. 1a). 293 T cells were transfected with four different lentiviral cDNA pools (#65, #50, #70 and #110). Subsequently, UT-7/EPO cells were transduced with these four different lentivirus library pools and cultured for four weeks in semi-solid media in the absence of EPO. Clones that acquired the ability to proliferate in the absence of EPO were identified and analyzed. Lentiviral-transduced cells were identified by Venus fluorescence that was encoded by the lentiviral vector. UT-7/EPO cells that were cultured in the absence of EPO failed to generate colonies, whereas these cells generated equal numbers of colonies when cultured in semi-solid media containing EPO (data not shown). When UT-7/EPO cells that had been transduced with the lentiviral library (6×10^5 cDNAs) were cultured in the absence of EPO, 22 EPO-independent colonies formed (Fig. 1b–c).

Next, to identify the cDNAs responsible for this EPO-independent proliferation, genomic DNA was isolated from each colony, and the integrated cDNAs were PCR amplified using lentivirus-specific primers (Fig. 1d). Agarose gel electrophoresis of the PCR products for each colony showed multiple bands of different sizes (Fig. 1d, lanes 2 and 3). This amplification was specific because untransduced UT-7/EPO cells did not yield any PCR products (lane 1), and a PCR product of the expected size was amplified from UT-7/EPO cells transduced with a lentivirus encoding green fluorescent protein (GFP) (lane 4).

Candidate Genes Identified from UT-7/EPO Cells Transduced with Human FL Lentiviral cDNA Library

The PCR products from the first round of screening were sequenced to identify the candidate genes that were expressed during erythropoiesis. Each pool contained a different number of inserted genes (Table 1). From the first screening, the following genes were identified as candidates that contributed to the growth of EPO-independent colonies; *FHS* and *FLC* encoding iron-binding proteins; the vitamin D-binding protein *GC*; the plasma protein receptor *ASGR2*; the vasoregulator *AGT*; estrogen-responsive protein *EBAG9*; the collagen *COL18A1*; the ribosomal protein *RPL10*; the kinase *PDPK1*; *ABI-2*, a kinase-binding protein; *APOA-1*, *APOE*, *APOJ* and *SLC27A2*, all of which encode lipid metabolism-related proteins; the anti-apoptotic protein *BCL2-like1*; and *1-8D*, encoding a protein of unknown function.

Among the integrated genes, some (*AGT*, *FHS*, *1-8D*, *FLC* and *GC*) were inserted into the host genome as a full-length coding sequence (CDS). As a result, these genes produced functional proteins that could be expressed in UT-7/EPO cells and lead to colony formation in the absence of EPO. Other genes (*BCL2-like1*, *APOA-1*, *PDPK1*, *FGL1*, *APOE*, *SLC27A2* and *COL18A1*) were inserted as a partial CDS that lacked the 5′ first start codons but contained 3′ stop codons, indicating that these genes were translated from a secondary start codon to the stop codon to yield partial proteins. As a result, functional proteins may be expressed in UT-7/EPO cells, leading to colony formation in the absence of EPO. The remaining inserted genes (*EBAG9*, *ABI-2*, *ASGR2* and *APOJ*) consisted of only a

Table 2 Gene specific primers for candidate genes in mice

Agt	5′	AGTGGGAGAGGTTCTCAATAGCA
	3′	GACGTGGTCGGCTGTTCCT
Ebag9	5′	GCAGCTACACAAGACATGCCTTT
	3′	TCCCACGCATTGCTATTTTCT
Bcl2-like1	5′	GGCTGGGACACTTTTGTGGAT
	3′	AAGCGCTCCTGGCCTTTC
Apoa-1	5′	GACAGCGGCAGAGACTATGTGT
	3′	AGGAGATTCAGGTTCAGCTGTTG
Fhs	5′	GCATGCCGAGAAACTGATGA
	3′	TCACGGTCTGGTTTCTTTATATCCT
Pdpk1	5′	TTCTTGGCGAGGGCTCTTT
	3′	CATATTCTCTGGAAGTGGCCAGTT
Abi-2	5′	GCGGGTGGCCGACTACT
	3′	TCTTCTAGGGCTCGCTGCTT
Apoe	5′	AGCTGCAGAGCTCCCAAGTC
	3′	TTACTTCCGTCATAGTGTCCTCCAT
1-8d	5′	CCTGGGCTTCGTTGCCTAT
	3′	CACATCGCCCACCATCTTC
Asgr2	5′	GGAGGAGAAGCAGCAACAGCTA
	3′	TGGGAAGTGCTTCAGGTGAAA
Flc	5′	CGGGCCTCCTACACCTACCT
	3′	GCCACGTCATCCCGATCA
Slc27a2	5′	CAACACACCGCAGAAACCAA
	3′	CCATTTCCCAGGGCTTTTTT
Rpl10	5′	TTCCATGTCATCCGTATCAACAA
	3′	CCCTGTCTGGAGCCTGTCA
Col18a1	5′	GCAGAGCCAGAGAATGTTGCT
	3′	CCCGACGTGAGGGTCATC
Apoj	5′	GGTCGGCCAGCAGCTAGAG
	3′	CGCCGTTCATCCAGAAGTAGA
Gc	5′	GGATCCTGCTGTACTTCTGCAA
	3′	TGCTTCATCTGGAGTCTCTCCTT

partial CDS without an open reading frame (ORF). These genes were translated from the shifted reading frame of the original mRNA and produced proteins of uncertain function. However, these genes resulted in UT-7/EPO colony formation in the absence of EPO. All of the 17 candidate cDNAs with full-length, partial or matched ORFs or partial but non-matched ORFs were examined in a secondary screen to identify specific genes that were involved in terminal erythroid maturation.

Expression of EPO-independent Growth-inducing Genes in Mouse FL Erythroid Populations

To determine which candidate genes obtained from first screen are critical for primary erythroid cell maturation, we performed a second screen to analyze gene expression during erythroid development. We used mouse fetuses for the second screen since mouse fetal samples are easier to obtain and use than human samples. The mouse homologues of these candidate genes were identified and the expression of the candidate genes was analyzed by RT-PCR using gene-specific primers (Table 2).

First, gene expression was assessed in samples from E10.5 whole embryos (WE) and E12.5 FL. All candidate genes were expressed in E12.5 FL with the exception of *Asgr-2,* which was eliminated as a gene of interest (Fig. 2). *Ebag9* and *Col18a1* expression was lower in the FL than in the whole E10.5 embryos, while *Fhs* and *Gc* had the opposite expression pattern with higher expression in the FL samples.

Next, we analyzed candidate gene expression in a series of FL-derived hematopoietic populations ranging from uncommitted hematopoietic stem cells (HSCs) to mature erythrocytes as determined by the expression of the surface markers CD45, Sca-1, c-Kit, CD71 and Ter119 (Fig. 3a). The following criteria were used to identify each hematopoietic population: (1) CD45+/Sca-1+/c-Kit+ cells represent HSCs; (2) c-Kit+ (Sca-1-/c-Kit+/CD71-/Ter119-) cells are BFU-E; (3) c-Kit+/CD71+ (Sca-1-/c-Kit+/CD71+/Ter119-) cells are committed erythroid progenitor cells or CFU-E; (4) CD71+/Ter119+ (Sca-1-/c-Kit-/CD71+/Ter119+) cells are proerythroblasts; and (5) Ter119+ (Sca-1-/c-Kit-/CD71-/Ter119+) cells represent mature erythroblasts and erythrocytes (Fig. 3a) [14, 15].

The mRNA expression of some candidate genes (*Abi-2*, *Slc27a2*) was higher in HSCs and gradually decreased throughout erythroid cell maturation (Fig. 3b). The expression of other candidate genes (*Pdpk1*, *Fhs*, *Flc*, *Rpl10*, *Ebag9* and *Apoe*) increased from HSCs to erythroblasts and then gradually decreased from erythroblasts to mature erythrocytes. *Bcl2l1* expression was low in HSCs and gradually increased. *Apoa-1* was highly expressed in

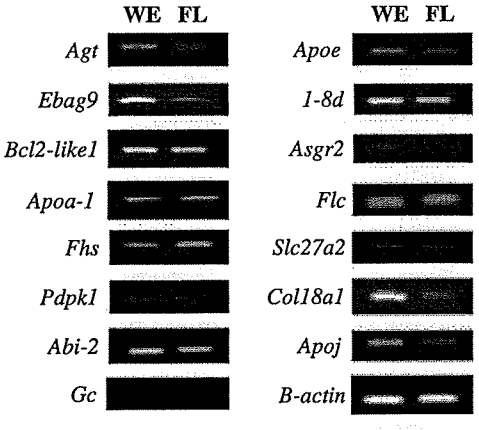

Fig. 2 Expression of candidate erythroid genes in developing mouse embryos. RT-PCR analyses of candidate genes in mouse embryos. We used RT-PCR to examine the expression patterns of the mouse homologues of each candidate gene in 10.5 dpc whole embryos (WE) and 12.5 dpc FL in ICR mouse embryos

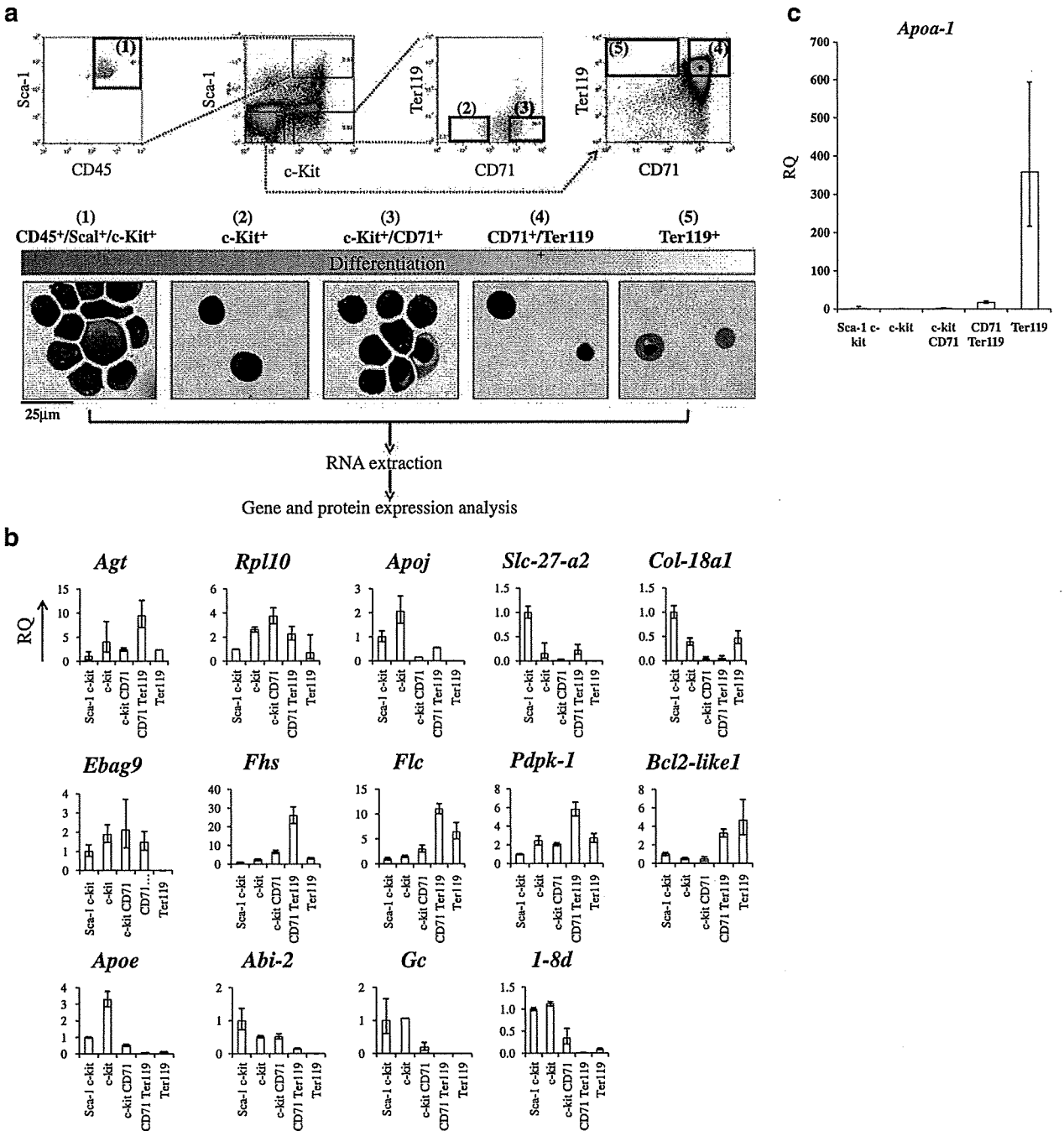

Fig. 3 Isolation of maturing erythroid populations from mouse FL cells. **a** Hematopoietic stem cells and maturing erythroid populations were isolated from 12.5 dpc mouse FL based on the expression of the surface markers CD45 (common leukocyte antigen), Sca-1 (stem cell antigen-1), c-Kit (stem cell factor receptor), CD71 (transferrin receptor) and Ter119 (Glycophorin A-associated antigen). The cytospins of each cellular fraction were prepared for May-Grunwald-Giemsa staining. As erythroid cells mature, the cell size decreased and finally the erythrocytes were enucleated. **b** mRNA expression patterns of candidate genes during erythroid cell maturation. The mRNA levels of candidate genes in maturing erythroid populations were analyzed by qRT-PCR. Total RNA was isolated from FL cells of 12.5 dpc embryos (Bars represent the means ± SD). The horizontal axes indicate the HSC fraction and the erythroid cell stage. Erythroid cell development proceeds from left to right. The vertical axes indicate the relative quantitation (RQ) of mRNA expression with the Sca-1$^+$/c-Kit$^+$ cell fraction set at an RQ value of 1. **c** The expression of mouse *Apoa-1* was significantly increased in the terminal maturation stages (Ter119$^+$ cell fraction) of cells obtained from 12.5 dpc FL

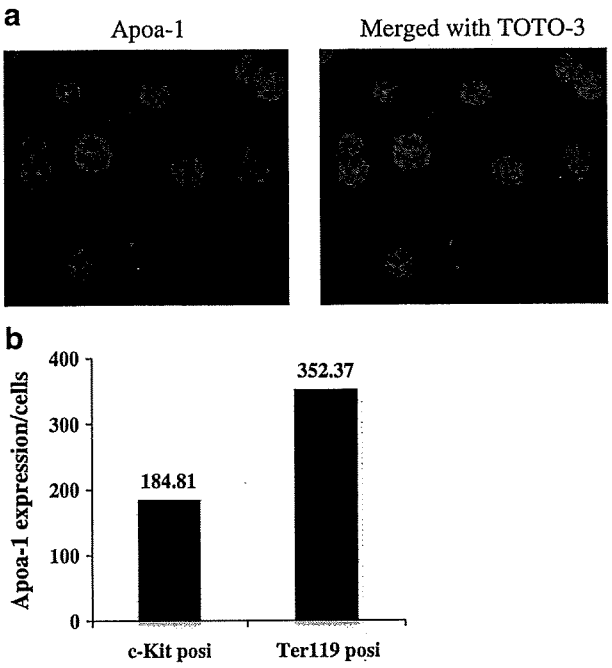

Fig. 4 Apoa-1 protein expression in mouse FL cells. **a** Immunohistochemistry. Ter119-positive cells from 12.5 dpc FL cells were cytospun and stained with an anti-mouse Apoa-1 antibody. Apoa-1-positive cells (*red*) were observed in 12.5 dpc FL cells. Nuclei were stained with TOTO3 (*blue*). **b** ELISA. c-Kit-positive cells and Ter119-positive cells from 12.5 dpc FL cells were sorted. Protein was extracted from each fraction and then analyzed by a sandwich ELISA. The expression levels of the mouse Apoa-1 proteins are shown for each fraction

Ter119-positive mature erythrocytes (Fig. 3c). The mRNA levels of *Apoa-1* increased approximately 350-fold, respectively, in the Ter119-positive cell population compared to the HSC population, suggesting that both of these genes are involved in the terminal maturation of erythroid cells.

Expression of the Apoa-1 Protein in Mouse FL Cells

To determine whether Apoa-1 is expressed at the protein level in mouse erythroid cells, immunohistochemical analyses were performed. Ter119-positive cells in mouse FL cells expressed the Apoa-1 protein (Fig. 4a). A sandwich enzyme-liked immunosorbent assay (ELISA) was also performed to quantitatively analyze the protein expression level in 12.5 dpc mouse FL cells. Because it is difficult to extract sufficient amounts of protein for an ELISA from individually fractionated cells in the populations shown in Fig. 3a, we compared the following two groups to analyze protein expression: c-Kit-positive cells, namely ((1)+(2)+(3) in Fig. 3) and Ter119-positive cells or ((4)+(5) in Fig. 3). As shown in Fig. 4b, Apoa-1 protein expression was approximately two-fold higher in Ter119-positive cells than c-Kit-positive cells, indicating that Apoa-1 expression correlates with terminal erythroid maturation at the protein level.

APOA-1 Expression in Human Peripheral Blood

To determine whether APOA-1 is useful as a terminal erythroid marker in human samples, we examined mRNA

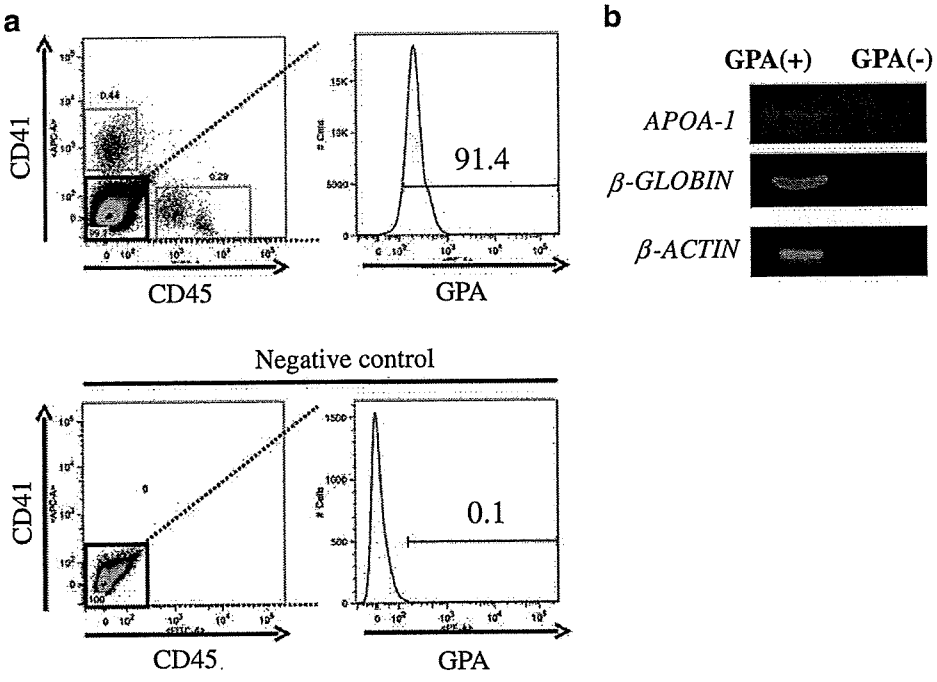

Fig. 5 *APOA-1* gene expression in human peripheral blood. **a** Erythrocytes and reticulocytes were isolated from human peripheral blood based on the expression of surface markers CD41 (integrin IIb), CD45 (common leukocyte antigen) and GPA (glycophorin A). **b** RT-PCR was performed to assess expression of human *APOA-1*. Human *β-GLOBIN* expression was analyzed to confirm that erythrocytes and reticulocytes had been isolated by flowcytometry. *APOA-1* was expressed in human peripheral blood

expression in human peripheral blood (PB) erythrocytes and reticulocytes. Erythrocytes and reticulocytes were isolated from peripheral blood by flow cytometry based on the expression of the cell surface markers glycophorin A (GPA), CD41 and CD45. In the PB, 91.4% of the CD41-/CD45-cells were positive for GPA (Fig. 5a). Reverse transcriptase PCR (RT-PCR) analysis showed that *β-GLOBIN* was expressed in GPA-positive cells, indicating that erythrocyte and reticulocyte mRNA was successfully extracted from the PB (Fig. 5b). Furthermore, *APOA-1* mRNA was expressed in the same fraction, demonstrating that this molecules can be used as a potential marker for terminal erythroid maturation in humans as well as mice.

Discussion

The goal of this study was to identify novel genes that are expressed during the terminal, EPO-independent maturation of erythroid cells. A two-step approach consisting of a lentiviral human FL cDNA library screen followed by an analysis of the gene expression patterns during erythropoiesis was performed to efficiently identify target genes.

This strategy had two clear advantages. First, it is important to establish a screening system that can detect erythropoiesis-related genes in an EPO-independent manner. A human FL cDNA library can be screened to identify novel genes. In this study, UT-7/EPO cells were transduced with a FL cDNA expression lentiviral library to detect genes that generate erythroid colonies in semi-solid medium in the absence of the EPO signaling pathway. Second, this screen could examine the effects of a large number (6×10^5) of genes on erythroid maturation. As humans are estimated to have approximately $2–3\times10^4$ genes, our screening encompassed a sufficient number of human cDNAs.

BCL2-like1 (BCL2L1) was one of the candidate genes identified in the first screen. *BCL2L1* encodes an anti-apoptotic protein that plays an important role in erythropoiesis in the absence of EPO [16]. Therefore, the results of our first screen strongly indicated that this system could be used to identify EPO-independent erythropoiesis-related genes. Other candidate genes included *FHS* and *FLC*, which encode iron-binding proteins, and *APOE, APOA-1, APOJ* and *SLC27A2,* which encode lipid metabolism-related proteins. Both iron and lipid metabolism are important cellular processes that regulate erythroid maturation [17–19]. We also identified a number of genes that were not previously implicated in erythropoiesis, including a vitamin D-binding protein (*GC*), vasoregulator (*AGT*), estrogen-responsive gene (*EBAG9*), collagen type 18 (*COL18A1*), ribosomal protein (*RPL10*) and several kinase-related proteins (*PDPK1* and *ABI-2*).

We also specifically identified a gene that was upregulated in the terminal stages of erythrocyte maturation. The identification of this gene is significant because very few molecular markers can be used to examine this stage of erythropoiesis. The candidate gene, *APOA-1*, was particularly interesting. APOA-1 is a major protein component of high-density lipoprotein (HDL) in the plasma and promotes the efflux of cholesterol from the tissues to the liver for excretion [20]. APOA-1 is a cofactor for lecithin cholesterol acyltransferase (LCAT), which is responsible for the formation of most plasma cholesteryl esters.

APOA-1 interacts with the ATP-binding cassette transporter ABCA1 (member 1 of human transporter sub-family ABCA) [21]. A recent report demonstrated that the APOA-1/ABCA1 pathway functions as an anti-inflammatory receptor by activating Janus Kinase 2 (JAK2)/Signal Transducers and Activation of Transcription3 (STAT3) in macrophages [22]. JAK2/STAT3 and/or JAK2/STAT5 are central signal pathways in erythroid cells [23]. Therefore, APOA-1/ABCA1 may activate the JAK2/STAT3 and/or JAK2/STAT5 pathway during the terminal maturation of erythroid cells.

It is intriguing to note that defects in APOA-1 are associated with low HDL levels observed in HDL deficiency type 1, which includes analphalipoproteinemia or Tangier disease. In Tangier disease patients, APOA-1 fails to associate with HDL. This inability to bind HDL is likely due to the faulty conversion of pro-APOA-1 molecules into mature chains, either due to a defect in the converting enzyme or a specific structural defect [24–26]. Furthermore, red blood cells in patients with Tangier disease have stomatocytosis and hemolytic anemia [27]. Moreover, patients with beta-thalassemia major as well as sickle cell disease have lower levels of APOA-1 in their plasma than healthy controls [28]. This abnormal erythrocyte morphology could be partially explained by a recent report by Holm TM et al., which showed that knockout mice with defects in the high-density lipoprotein receptor SR-BI have abnormal erythrocyte morphology. On the other hand, the fractional catabolic rate (FCR) for APOA-1 was significantly increased in patients with myeloproliferative disorders, including polycythemia vera, compared with healthy controls [29]. Therefore, accelerated red blood cell production could be also supported by increased APOA-1 catabolism. Further studies including both in vitro and/or in vivo analyses of APOA-1 knockouts are necessary to demonstrate the direct importance of APOA-1 in the maturation of red blood cells.

This study is the first to report that APOA-1 is a novel molecular marker for terminal erythroid maturation from HSC. In combination with Ter119 antigen or glycophorin A antigen, this molecule can potentially be used to identify mature erythrocytes in in vitro cultured erythroid cell

sources such as ES or iPS cells. It will be necessary to further investigate whether APOA-1 plays pivotal roles in erythroid cell maturation and is a useful maturation marker.

Acknowledgements The authors would like to thank Chiyo Mizuochi, Yuka Horio, Tatsuya Sasaki and Michiko Ushijima at Kyushu University for excellent technical assistance. This work was supported by a grant from the Project for Realization of Regenerative Medicine from the Ministry of Education, Culture, Sports, Science and Technology and by a grant from the BASIS project from the Ministry of Education, Culture, Sports, Science and Technology. T. Inoue is supported by research fellowships from the Japan Society for the Promotion of Science for Young Scientists.

Disclosures The authors indicate no potential conflicts of interest.

References

1. Weissman, I. L. (2000). Stem cells: units of development, units of regeneration, and units in evolution. *Cell, 100*, 157–168.
2. Mikkola, H. K., & Orkin, S. H. (2006). The journey of developing hematopoietic stem cells. *Development, 133*, 3733–3744.
3. Medvinsky, A., & Dzierzak, E. (1996). Definitive hematopoiesis is autonomously initiated by the AGM region. *Cell, 86*, 897–906.
4. Sugiyama, D., & Tsuji, K. (2006). Definitive hematopoiesis from endothelial cells in the mouse embryo; a simple guide. *Trends in Cardiovascular Medicine, 16*, 45–49.
5. Ema, H., & Nakauchi, H. (2000). Expansion of hematopoietic stem cells in the developing liver of a mouse embryo. *Blood, 95*, 2284–2288.
6. Palis, J. (2008). Ontogeny of erythropoiesis. *Current Opinion in Hematology, 15*, 155–161.
7. McGrath, K., & Palis, J. (2008). Ontogeny of erythropoiesis in the mammalian embryo. *Current Topics in Developmental Biology, 82*, 1–22.
8. Hiroyama, T., Miharada, K., Sudo, K., Danjo, I., Aoki, N., & Nakamura, Y. (2008). Establishment of mouse embryonic stem cell-derived erythroid progenitor cell lines able to produce functional red blood cells. *PLos One, 3*, e1544.
9. Kina, T., Ikuta, K., Takayama, E., et al. (2000). The monoclonal antibody TER-119 recognizes a molecule associated with glycophorin A and specifically marks the late stages of murine erythroid lineage. *British Journal Haematology, 109*, 280–287.
10. Zhang, J., Socolovsky, M., Gross, A. W., & Lodish, H. F. (2003). Role of Ras signaling in erythroid differentiation of mouse fetal liver cells: functional analysis by a flow cytometry-based novel culture system. *Blood, 102*, 3938–3946.
11. Kurita, R., Sasaki, E., Yokoo, T., et al. (2006). Tal1/Scl gene transduction using a lentiviral vector stimulates highly efficient hematopoietic cell differentiation from common marmoset (Callithrix jacchus) embryonic stem cells. *Stem Cells, 24*, 2014–2022.
12. Kurita, R., Oikawa, T., Okada, M., et al. (2008). Construction of a high-performance human fetal liver-derived lentiviral cDNA library. *Molecular and Cellular Biochemistry, 319*, 181–187.
13. Komatsu, N., Yamamoto, M., Fujita, H., et al. (1993). Establishment and characterization of an erythropoietin-dependent subline, UT-7/Epo, derived from human leukemia cell line, UT-7. *Blood, 82*, 456–464.
14. Suzuki, N., Suwabe, N., Ohneda, O., et al. (2003). Identification and characterization of 2 types of erythroid progenitors that express GATA-1 at distinct levels. *Blood, 102*, 3575–3583.
15. Walkley, C. R., & Orkin, S. H. (2006). Rb is dispensable for self-renewal and multilineage differentiation of adult hematopoietic stem cells. *Proceedings of the National Academy of Sciences of the United States of America, 103*, 9057–9062.
16. Dolznig, H., Habermann, B., Stangl, K., et al. (2002). Apoptosis protection by the Epo target Bcl-X(L) allows factor-independent differentiation of primary erythroblasts. *Current Biology, 12*, 1076–1085.
17. Gelvan, D., Fibach, E., Meyron-Holtz, E. G., & Konijn, A. M. (1996). Ferritin uptake by human erythroid precursors is a regulated iron uptake pathway. *Blood, 88*, 3200–3207.
18. Meyron-Holtz, E. G., Vaisman, B., Cabantchik, Z. I., et al. (1999). Regulation of intracellular iron metabolism in human erythroid precursors by internalized extracellular ferritin. *Blood, 94*, 3205–3211.
19. Holm, T. M., Braun, A., Trigatti, B. L., et al. (2002). Failure of red blood cell maturation in mice with defects in the high-density lipoprotein receptor SR-BI. *Blood, 99*, 1817–1824.
20. Breslow, J. L., Ross, D., McPherson, J., et al. (1982). Isolation and characterization of cDNA clones for human apolipoprotein A-I. *Proceedings of the National Academy of Sciences of the United States of America, 79*, 6861–6865.
21. Fitzgerald, M. L., Morris, A. L., Rhee, J. S., Andersson, L. P., Mendez, A. J., & Freeman, M. W. (2002). Naturally occurring mutations in the largest extracellular loops of ABCA1 can disrupt its direct interaction with apolipoprotein A-I. *Journal of Biological Chemistry, 277*, 33178–33187.
22. Tang, C., Liu, Y., Kessler, P. S., Vaughan, A. M., & Oram, J. F. (2009). The macrophage cholesterol exporter ABCA1 functions as an anti-inflammatory receptor. *Journal of Biological Chemistry, 47*, 32336–32343.
23. Richmond, T. D., Chohan, M., & Barber, D. L. (2005). Turning cells red: signal transduction mediated by erythropoietin. *Trends in Cell Biology, 15*, 146–155.
24. Zannis, V. I., Lees, A. M., Lees, R. S., & Breslow, J. L. (1982). Abnormal apoprotein A-I isoprotein composition in patients with Tangier disease. *Journal of Biological Chemistry, 257*, 4978–4986.
25. Gordon, J. I., Sims, H. F., Lentz, S. R., Edelstein, C., Scanu, A. M., & Strauss, A. W. (1983). Proteolytic processing of human preproapolipoprotein A-I. A proposed defect in the conversion of pro A-I to A-I in Tangier's disease. *Journal of Biological Chemistry, 258*, 4037–4044.
26. Schmitz, G., Assmann, G., Rall, S. C., Jr., & Mahley, R. W. (1983). Tangier disease: defective recombination of a specific Tangier apolipoprotein A-I isoform (pro-apo A-i) with high density lipoproteins. *Proceedings of the National Academy of Sciences of the United States of America, 80*, 6081–6085.
27. Reinhart, W. H., Gossi, U., Butikofer, P., et al. (1989). Haemolytic anaemia in analpha-lipoproteinaemia (Tangier disease): morphological, biochemical, and biophysical properties of the red blood cell. *British Journal Haematology, 72*, 272–277.
28. Sasaki, J., Waterman, M. R., & Cottam, G. L. (1986). Decreased apolipoprotein A-I and B content in plasma of individuals with sickle cell anemia. *Clinical Chemistry, 32*, 226–227.
29. Ginsberg, H. N., Le, N. A., & Gilbert, H. S. (1986). Altered high density lipoprotein metabolism in patients with myeloproliferative disorders and hypocholesterolemia. *Metabolism, 35*, 878–882.

jgm1467

RESEARCH ARTICLE

THE JOURNAL OF GENE MEDICINE
J Gene Med 2010; **12**: 000–000.
Published online in Wiley InterScience (www.interscience.wiley.com) **DOI:** 10.1002/jgm.1467

Carrier cell-mediated cell lysis of squamous cell carcinoma cells by squamous cell carcinoma antigen 1 promoter-driven oncolytic adenovirus

Katsuyuki Hamada[1]*
Ting Zhang[2]
Junzo Desaki[3]
Koh-ichi Nakashiro[2]
Hiroshi Ito[4]
Kenzaburo Tani[5]
Yoshiyuki Koyama[6]
Hiroyuki Hamakawa[2]

[1]*Department of Obstetrics and Gynecology, Ehime University, Ehime, Japan*

[2]*Department of Oral and Maxillofacial Surgery, Ehime University, Ehime, Japan*

[3]*Department of Anatomy, Ehime University, Ehime, Japan*

[4]*Animal Medical Center, Tokyo University of Agriculture and Technology, Tokyo, Japan*

[5]*Department of Advanced Molecular and Cell Therapy, Kyushu University Hospital, Kyushu University, Fukuoka, Japan*

[6]*Department of Textile Science, Otsuma Women's University, Tokyo, Japan*

*Correspondence to:
Katsuyuki Hamada, Department of Obstetrics and Gynecology, School of Medicine, Ehime University, Shitsukawa, Toon, Ehime 791-0295, Japan.
E-mail: hamakatu@m.ehime-u.ac.jp

Received: 5 October 2009
Revised: 1 February 2010
Accepted: 27 April 2010

Abstract

Background The squamous cell carcinoma antigen (SCCA) serves as a serological marker for squamous cell carcinomas. Molecular cloning of the *SCCA* genomic region has revealed the presence of two tandemly arrayed genes: *SCCA1* and *SCCA2*. *SCCA1* gene is up-regulated in squamous cell carcinoma cells. We analyzed the proximal region of the *SCCA1* promoter and the antitumor effect of oncolytic adenovirus driven by the *SCCA1* promoter in squamous cell carcinoma cells.

Methods The *SCCA1* promoter was analyzed by dual luciferase assay and substituted with the *E1A* promoter to construct the oncolytic adenovirus to determine the squamous cell carcinoma-specific cell lysis.

Results Deletion analysis of *SCCA1* promoter identified a 175-bp core promoter region and an enhancer region at −525 to −475 bp upstream of the transcription start site. The transcriptional activity of the *SCCA1* promoter was up-regulated in squamous cell carcinoma cells. Five tandem repeats of enhancer increased *SCCA1* promoter activity by four-fold. Oncolytic adenovirus driven by this *SCCA1* enhancer-promoter complex specifically killed squamous cell carcinoma cells *in vitro* and *in vivo*. A549 carrier cells infected with the oncolytic adenovirus induced complete regression of syngeneic squamous cell carcinoma cell tumor by overcoming immunogenicity and adenovirus-*mGM-CSF* augmented the antitumor effect of carrier cells.

Conclusions *SCCA1* was up-regulated in squamous cell carcinoma cells and oncolytic adenovirus driven by *SCCA1* promoter specifically killed these cells. These findings suggest that *SCCA1* promoter is a potential target of gene therapy for squamous cell carcinoma. Copyright © 2010 John Wiley & Sons, Ltd.

Keywords adenovirus; cervical cancer; oncolytic carrier cell; promoter; squamous cell carcinoma; squamous cell carcinoma antigen 1

Introduction

Squamous cell carcinoma antigen (SCCA) is a circulating tumor marker for squamous cell carcinoma, especially that of cervix, head and neck, lung, and oesophagus [1]. Elevated circulating levels of SCCA are not detected in patients with adenocarcinomas of the uterus, ovary, or breast [2]. Several studies have shown that increased serum SCCA levels are correlated with the extent of disease in patients with squamous cell carcinoma [2–4]. Higher

SCCA levels are also indicative of deep tumor infiltration and lymph node involvement [5,6]. Moreover, measurement of post-treatment SCCA levels is useful for monitoring the response to therapy as well as for predicting tumor recurrence and metastasis. SCCA protein has been isolated from a metastatic, cervical squamous cell carcinoma [2]. Molecular cloning of the *SCCA* genomic region revealed the presence of two tandemly arrayed genes: *SCCA1* and *SCCA2*. Although SCCA1 and SCCA2 are almost identical members of the serpin superfamily, the significant differences in their reactive site loops suggest that SCCA1 is a papain-like cysteine proteinase inhibitor, whereas SCCA2 is a chymotrypsin-like serine proteinase inhibitor [7].

Previous studies have reported the cloning and characterization of the promoter region of *SCCA1* [8] and *SCCA2* [9]. *SCCA1* gene expression and promoter activity is up-regulated in squamous cell carcinoma cells compared to keratinocyte and adenocarcinoma cells [8,10]. *SCCA2* gene expression and promoter activity are also increased in squamous cell carcinoma cells compared to normal and adenocarcinoma cells, although the *SCCA1* gene expression and promoter activity are higher than the *SCCA2* gene expression in almost all squamous carcinoma cells and tissues [8,10]. These findings suggest that *SCCA1* promoter may be a potential target of gene therapy for squamous cell carcinoma. Although the *SCCA2* promoter has been introduced into E1-deleted adenovirus to transduce an apoptotic gene in lung cancer [11], use of *SCCA1* promoter-driven adenovirus to treat squamous cell carcinoma has not yet been reported. We found that up to five consecutive tandem-repeat enhancer elements significantly increased *SCCA1* promoter activity. Oncolytic adenovirus AdE3-*SCCA1* was constructed by replacement of adenovirus *E1A* promoter with this tandem-repeat enhancer and promoter complex and specifically killed squamous cell carcinoma cells.

Materials and methods

Cell lines and culture conditions

Human non-small cell lung cancer A549, cervical squamous cell carcinoma SKGIIIa and gastric cancer AGS cells were obtained from the Japanese Collection of Research Bioresources Cell Bank (Osaka, Japan). Human ovarian carcinoma HEY and 2774 cells were obtained from Dr G. Mills, murine squamous cell carcinoma SCC7 cells were obtained from Dr L. Milas, and human non-small cell lung cancer H1299 cells were obtained from Dr J. A. Roth (The University of Texas, MD Anderson Cancer Center, TX, USA). Normal human keratinocyte SV, HPK, NHK and K42 cells and normal human fibroblast F27 cells were established by Dr K. Hashimoto (Ehime University, Japan). Normal human fibroblast NF and ovarian fibroblast NOE cells were established in our laboratory. Human umbilical vein endothelial HUVEC cells was obtained from Cambrex Bio Science Walkersville Inc. (Walkersville, MD, USA). Human cervical squamous cell carcinoma HT-III, C4I, C4II and CaSki cells, and human cervical adenocarcinoma HeLa cells, were obtained from the American Type Culture Collection (Rockville, MD, USA).

Cells were maintained in a humidified 5% CO_2/95% air incubator at 37 °C. All cell lines, except NHK, K42 and HUVEC cells, were grown in RPMI medium supplemented with 10% heat-inactivated fetal bovine serum. NHK and K42 cells were grown in MCDB153 (Nissui Co., Tokyo, Japan) with bovine hypothalamus extract. HUVEC cells were grown in EBM-2 (Cambrex, Baltimore, MD, USA)

Construction of the AdE3-*SCCA1* vector

The pXC1 plasmid has adenovirus 5 sequences from nucleotides 22–5790 containing the *E1* gene (Microbix Biosystems Inc., Toronto, Canada). A unique *AgeI* site was introduced at nucleotide position 404 after deletion between nucleotides 404 and 552 to generate the plasmid pXC1-404-*AgeI*. The *SCCA1* promoter was ligated to pXC1-404-*AgeI* plasmid to obtain pXC1-*SCCA1*. To construct the AdE3-*SCCA1* virus, homologous recombination was performed between pXC1-*SCCA1* plasmid and the right hand side of pBHGE3 adenovirus DNA containing the *E3* region in 293 cells by a standard technique [12]. To construct the wild-type adenovirus AdE3, homologous recombination was performed between pXC1 and pBHGE3 in 293 cells. The replication defective *E1*-deleted Ad5CMV-*LacZ* virus was used as control adenovirus. All viruses were purified with double CsCl gradients using standard methods, and titered by standard spectrophotometry and plaque assay [12].

Enzyme-linked immunosorbent assay (ELISA)

Each cell was seeded at 4×10^6 cells into 100-mm culture dishes and incubated for 2 days with 10 ml of culture medium. Each cell line was cultured in triplicate dishes. Supernatants were obtained from culture medium in each dish, centrifuged for 5 min at 3000 r.p.•m. at room temperature, and assayed to detect SCCA protein. An ELISA for SCCA (IMx SCC.•DAINAPACK™; Dainabot Co., Tokyo, Japan) was used to evaluate the concentrations of SCCA protein in medium. Medium samples (2 ml) were concentrated ten-fold by centrifugation with a Centricon-10 (Millipore Corp., Bedford, MA, USA). Concentrated samples (200 µl) were applied to an automatic assay apparatus (IMx analyzer; Dainabot Co.). The lower limit of detection with this ELISA system was 0.01 ng/ml. This assay system could detect both SCCA1 and SCCA2 proteins. The mean values of samples were determined in triplicates. All experiments were performed at least three times and gave similar results.

Real-time quantitative reverse transcriptase-polymerase chain reaction (RT-PCR)

One hundred ng RNA samples were used in RT and real-time PCR for RNA expression studies. A reverse transcriptase and real-time PCR reaction was carried out with the ABI prism 7700 sequence detection system (Applied Biosystems, Foster City, CA, USA) in a total volume of 50 μl that contained TaqMan one step RT-PCR master mix (Applied Biosystems), 0.3 μM of each forward and reverse primer, and 0.21 μM of MGB probe. The forward and reverse primer and MGB probe were: 5′-CCACCGCTGTAGTAGGATTCG-3′, 5′-GGAAAGGGTGATTACAATGGAACTC-3′ and 5′-ATCATCACCTACTTCAAC-3′ for *SCCA1* and 5′-CATGACC TGGAGCCACGG-3′, 5′-CCCTCCTCAGTGACCTCCAC-3′ and 5′-CTCTCAGTATCTAAAGTCCTAC-3′ for *SCCA2*. The reaction was performed with the following thermal cycling method: 30 min at 48 °C for reverse transcription, 5 min at 95 °C for AmpliTaq Gold activation, 15 s at 95 °C and 60 s at 60 °C for 40 cycles. *GAPDH* was chosen as a housekeeping gene to be tested as an endogenous control.

Assay for promoter activity

SCCA1 and *SCCA2* promoter fragments were inserted into the luciferase reporter vector PicaGene Basic, a promoterless and enhancerless vector (Toyo Ink MFG Co., Tokyo, Japan). The sequence of each insert was confirmed by an ABI PRISM 310 Genetic Analyzer (Applied Biosystems). Constructs containing *SCCA1* and *SCCA2* promoter sequences were fused to the *Luciferase* gene which were transfected into cells in the presence of Lipofectamine transfection reagent (Invitrogen, Carisbad, CA, USA), in accordance with manufacturer's instructions. Briefly, 1×10^5 cells seeded in a 12-well culture dish were exposed to transfection mixtures containing 1 μg of luciferase reporter plasmids and 0.2 μg of prenilla luciferase-herpes simplex virus thymidine kinase promoter control vector (Promega, Madison, WI, USA) at 37 °C for 48 h. Dual luciferase assays were performed in accordance with manufacturer's instructions.

Cell count assay

Cells were plated at a density of 5×10^3 cells/well in 12-well plates. Cells were infected with AdE3-*SCCA1* or AdE3. Culture medium alone was used as a mock infection control. After 15 days, cells were harvested and counted to determine the 50% growth inhibitory concentration (IC_{50}).

Inhibition of subcutaneous tumor growth *in vivo*

To determine inhibition of xenograftic subcutaneous tumor growth, AdE3-*SCCA1* was injected into subcutaneous tumors in female nude (*nu/nu*) mice (CLEA Japan Inc., Tokyo, Japan). In brief, 1×10^7 HT-III or H1299 cells in 100 μl of RPMI were injected into the left posterior flank of each mouse through an insulin syringe with a 27 1/2-gauge needle. Ten animals were used for each group. After 25 days, tumors with a diameter of 5–8 mm were established. Then 100 μl of AdE3 [1×10^{10} plaque-forming units (PFU)], AdE3-*SCCA1* (1×10^{10} PFU), Ad5CMV-*LacZ* (1×10^{10} PFU), or medium alone was injected intratumorally on days 0, 1, 2, 3, 4 and 5. The tumors were measured every 5 days with calipers in two perpendicular diameters. Tumor volume was calculated by assuming a spherical shape, with the average tumor diameter calculated as the square root of the product of cross-sectional diameters.

To determine inhibition of syngeneic subcutaneous tumor growth, murine SCC7 cells (1×10^6) were injected into the left posterior flank of female C3H/HeN mice (CLEA Japan Inc.) and AdE3-*SCCA1* was injected into subcutaneous tumors. Ten animals were used for each group. Medium alone; AdE3-*SCCA1* (1×10^{10} PFU) or A549 carrier cells (5×10^6) infected with AdE3-*SCCA1* at a multiplicity of infection (MOI) of 200; A549 carrier cells (5×10^6) infected with AdE3-*SCCA1* at a MOI of 200; and AxCA*mGM-CSF* at a MOI of 10 were injected into the tumors (5–8 mm in diameter) on days 0, 1 and 2. Mice were preimmunized with Ad-*LacZ* (1×10^{10} PFU) on day -21.

Animal studies have been approved by the Ehime University Review Board.

Statistical analysis

Values are the mean ± SD, and were examined with the unpaired *t*-test, Welch test and regression analysis. Survival data were plotted on Kaplan–Meier curves and examined with the log-rank test using the LIFETEST •procedure. $p < 0.05$ was considered statistically significant.

Results

Expression of SCCA protein

To determine the levels of expression of SCCA protein in human cervical squamous cell carcinoma cells, ELISA was performed in the medium of each cell line. SKGIIIa and HT-III cells secreted the highest concentrations of SCCA proteins into medium (Figure 1). The mean level of SCCA protein secretion by cervical squamous cell carcinoma cells was 15-fold greater than that of keratinocyte cells, 404-fold greater than that of normal non-keratinocyte